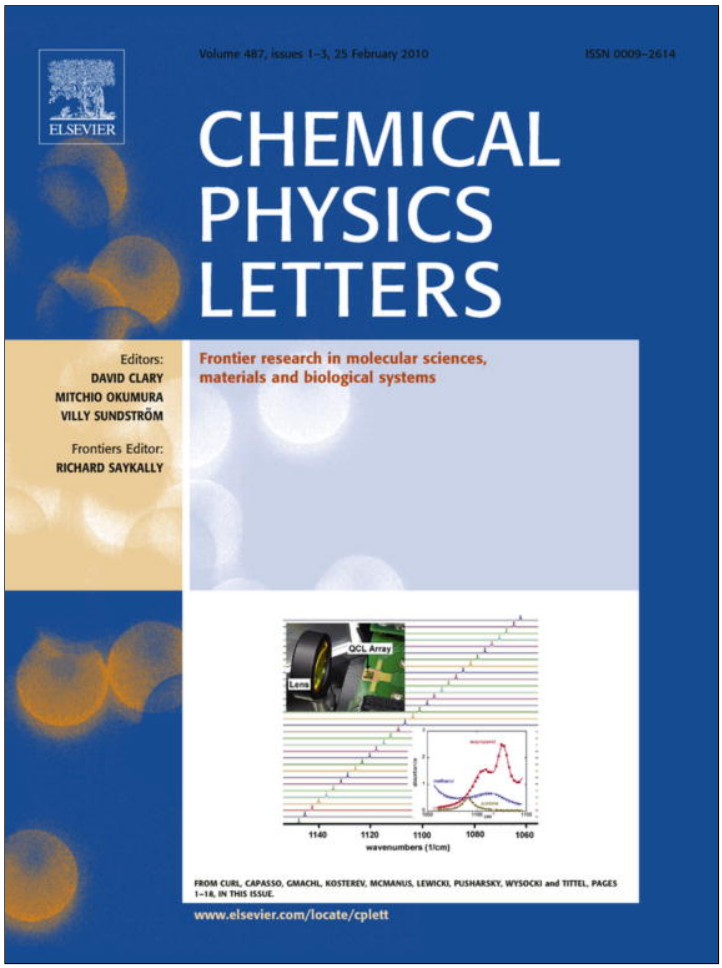

Chemical Physics Letters 487 (2010) 1–18

Contents lists available at ScienceDirect

Chemical Physics Letters

journal homepage: www.elsevier.com/locate/cplett

FRONTIERS ARTICLE

Quantum cascade lasers in chemical physics

Robert F. Curl [a,*], Federico Capasso [b], Claire Gmachl [c], Anatoliy A. Kosterev [d], Barry McManus [e], Rafał Lewicki [d], Michael Pusharsky [f], Gerard Wysocki [c], Frank K. Tittel [d]

[a] Department of Chemistry and Rice Quantum Institute, Rice University, Houston, TX 77005, USA
[b] School of Engineering and Applied Sciences, Harvard University, Cambridge, MA 02138, USA
[c] Department of Electrical Engineering, Princeton University, Princeton, NJ 08544, USA
[d] Department of Electrical and Computer Engineering, and Rice Quantum Institute, Rice University, Houston, TX 77005, USA
[e] Aerodyne Research Inc., Billerica, MA 01821, USA
[f] Daylight Solutions Inc., Poway, CA 92064, USA

ARTICLE INFO

Article history:
Received 22 December 2009
In final form 29 December 2009
Available online 4 January 2010

ABSTRACT

In the short space of 15 years since their first demonstration, quantum cascade lasers have become the most useful sources of tunable mid-infrared laser radiation. This Letter describes these developments in laser technology and the burgeoning applications of quantum cascade lasers to infrared spectroscopy. We foresee the potential application of quantum cascade lasers in other areas of chemical physics such as research on helium droplets, in population pumping, and in matrix isolation infrared photochemistry.

1. Introduction

For more than 80 years, infrared spectroscopy research and applications have played an increasingly important role in science and technology. Infrared laser spectroscopy began almost 40 years ago and has yielded many important results using a variety of tunable laser-based sources, particularly lead salt diodes, color center lasers, difference frequency generation, optical parametric oscillators, and sidebands on fixed frequency gas lasers. Quantum cascade lasers (QCLs) are a much more recent tunable laser source of infrared light.

The first quantum cascade laser was invented and demonstrated [1] at Bell Labs in 1994 by Faist, Capasso, Sivco, Hutchinson, and Cho. Twenty-three years earlier, laser amplification based on a similar emission principle had been proposed [2]. Since 1994, quantum cascade lasers developed rapidly so that by 2001 the field merited a review article [3] sixty-nine pages in length and in June 2002 a special issue of *IEEE Journal of Quantum Electronics*. Here we describe the status of quantum cascade laser technology and suggest new opportunities that these unique sources provide for infrared spectroscopy and its applications.

The first prototypes operated only in pulsed mode at a maximum temperature of 90 K. Advancements in band-engineering and waveguide designs led within a few years to many important achievements: pulsed room temperature operation, continuous wave (CW) and single mode operation, extension of the operating wavelength to values as short as 3.5 μm and as long as 19 μm, ultrashort pulse operation and to the first applications to spectroscopy and chemical sensing [4]. At first, QCLs had to be cooled to about 100 K to operate CW and operated multimode on several Fabry–Perot modes of the laser cavity formed by the cleaved ends of the laser chip. In 2002, CW room temperature operation was achieved [5] and since then continuous improvements in the design, material quality, fabrication and thermal management have led to record optical power of 34 W pulsed [6] and ≈3.0 W CW [7,8] at room temperature. The corresponding CW power efficiency for these Fabry–Perot cavity devices was 16.5% at 4.8 μm [7] and 13% at 4.6 μm [8]. A key factor in achieving such record CW performance was the use of high thermal conductivity diamond submounts. However, these are unsuitable for high reliability operation of high power lasers because they require the use of a soft indium solder, due to the large coefficient of thermal expansion (CTE) mismatch between diamond and the InP QCL substrate. Recently, comparable power performance was obtained from 4.6 μm QCLs using an aluminum nitride CTE-matched sub-mount and a hard AuSn solder, by optimizing the front facet reflectivity and cavity length [9]. This approach has led to commercially available (from Pranalytica Inc.) QCL high power systems for infrared countermeasures to protect aircraft from shoulder-held missiles, infrared target illuminators and beacons.

The development of single mode QCLs, essential for the narrow linewidth operation required for high resolution spectroscopy, started soon after the first QCL report by embedding in the laser cavity a grating that introduced distributed feedback (DFB) [10]. In a DFB laser, the cavity mode closest in wavelength to twice the effective grating period undergoes strong Bragg reflection and is therefore preferentially selected for lasing over modes at other wavelengths. These QC DFB lasers operating at a single frequency could be tuned over a few cm^{-1} to few tens of cm^{-1} by

* Corresponding author. Fax: +1 713 348 5155.
E-mail address: rfcurl@rice.edu (R.F. Curl).

0009-2614/$ - see front matter © 2010 Elsevier B.V. All rights reserved.
doi:10.1016/j.cplett.2009.12.073

varying current and temperature. Output powers were up to 100 mW in pulsed mode at room temperature at wavelengths in the 4.5 to ~10 μm range. QC DFB lasers quickly found application in trace gas monitoring. From the late 1990s until the present, many groups employed a number of spectroscopic techniques (long pass absorption, photoacoustic spectroscopy, cavity ring-down, intracavity absorption, magnetic rotation spectroscopy) to monitor a number of small molecules and a few larger molecules. However, the small tuning range and near-cryogenic temperatures required for CW operation of these first generation DFB lasers handicapped wider application.

The route to more applications required the production of QCLs with wider gain profiles that operated near-room temperature [11–21]. Besides being an enormous convenience, near-room temperature operation is required in order to make practical the optical coating of the laser end facets as well as the effective thermal management of the QCL. The QCL coatings will flake off upon cycling to low temperatures as a result of the difference in thermal expansion coefficients between the laser and coating. Through coating one end of the laser with a high reflection coating and the other with an antireflection coating, the laser can be incorporated into an external cavity. In the last few years, QCLs operating near-room temperature with broad gain profiles have become available and have been incorporated into external cavities to produce tuning ranges with a single QCL [22–27] of ~200 cm^{-1} CW and over 300 cm^{-1} pulsed with mW of very narrow band CW power. In a very recent development, an array of 32 DFB lasers on a single chip covering about 100 cm^{-1} in pulsed mode has been reported [28] making possible the creation of broadly tunable subminiature IR laser sources for spectroscopy. The tuning range of this source was recently increased to 220 cm^{-1} using a 24 laser array [29].

AlInAs/GaInAs grown on InP substrate is the material of choice for mid-infrared (mid-IR) QCLs. The original lasers were produced only using Molecular Beam Epitaxy (MBE), a technique in wide use for the manufacturing of many semiconductor devices. For growth of high-performance QCL heterostructures, several requirements must be satisfied. Foremost among these is the ability to form atomically abrupt interfaces between layers of nanometer or even sub-nm thickness. MBE is exemplary in this regard, however a properly designed MOCVD (Metallorganic Chemical Vapor Deposition) reactor can approach the interface abruptness associated with MBE. Low impurity background doping in the active region, in concert with controlled intentional-doping profiles in the injector regions, are also critical for QCLs in order to minimize the broadening of the laser transition and thus reduce the laser threshold. This requirement is not a problem for the AlInAs and GaInAs alloys grown by MOCVD. In addition, MOCVD may even offer some advantages over MBE for QCL growth. Among the anticipated benefits of MOCVD are stability of growth rate and composition over very long growth runs, the ease of achieving low oxygen contamination in aluminum-containing materials, the ability to grow thick InP cladding and burying layers, and the potential for very fast growth rates. On the other hand, it is expected that interface formation is more challenging for MOCVD; and also the requirement for organic precursors might lead to unacceptably high carbon background for some materials. This is the case for example of AlGaAs/GaAs alloys used for the growth of QCLs operating in far-infrared region, also known as Terahertz (THz) spectrum. Detailed studies of MOCVD grown QCLs operating at 4.6, 5.2 and 8.3 μm wavelength have shown that their pulsed and CW performance at room temperature is comparable to that of MBE QCLs [30,31]. Reliability tests indicate that MOCVD QCL devices operated without degradation for over 5000 h [30].

This review will be limited primarily to mid-IR QCLs. While there has been substantial progress in THz QCLs [32,33], their impact in spectroscopy has been as yet limited, unlike their counterparts in the mid-IR. The main reason is the very limited tuning range, in addition to the fact that they have to be cryogenically cooled. There indeed appear to be fundamental limits associated with the physics of transport in QCLs that will prevent room temperature operation, although Peltier cooled devices might be possible [32].

Advances in QCLs are revolutionizing infrared spectroscopy. Before showing how, we need to describe QCL design and their optimization for broad tunability, what frequency regions are accessible, what output powers can be obtained, and where lasers can be purchased.

2. Quantum cascade laser design and operation

Laser diodes emitting at wavelengths ranging from the near infrared to the visible are the workhorses of widespread technologies such as optical communications, optical recording (CD players, etc.), supermarket scanners, laser printers, fax machines and laser pointers. The operating principle of these lasers is fundamentally simple: electrons and holes are electrically injected into an active region made of semiconductor materials where they recombine, giving off laser photons of wavelength close to the bandgap of the active region. A corollary of this is that if one wishes to build diode lasers emitting at very different wavelengths one needs to choose materials with widely different bandgaps and therefore electronic and optical properties, for example quaternary alloys made of indium gallium phosphorous and arsenic for lasers emitting at telecom wavelengths around 1.3 and 1.5 μm and alloys containing gallium indium aluminum and nitrogen for blue emitting lasers. In spite of its simplicity and general nature, the diode laser principle has proven hard to extend to the mid-infrared while maintaining the same level of performance of its shorter wavelength counterparts. The reliance on the bandgap for light emission turns into a severely limiting factor at mid-infrared wavelengths, particularly across most of the molecular fingerprint region (2–20 μm) and beyond into the far-infrared. The reason is that as the bandgap shrinks in a semiconductor laser, its operation becomes much more critical in terms of the maximum operating temperature, temperature stabilization required to avoid thermal runaway effects and thermal recycling. To these problems one should add that, as the band gap shrinks, chemical bonds become weaker; this increased material 'softness' facilitates the introduction of defects during growth and device fabrication, making diode lasers less reliable and reducing device yields.

For example, semiconductor laser diodes made of lead salts [34,35] and emitting in the mid-IR, which have been used for many years in tunable laser spectroscopy, suffer from all of these limits. Lead–salt lasers have limited power (at most a few milliwatts of peak and continuous wave power), have a small continuous single-mode tuning range, and have yet to operate at room temperature. They also suffer from spectral degradation and reliability problems associated with thermal cycling.

2.1. Quantum cascade laser operating principle

The QCL overthrows the operating principle of conventional semiconductor lasers by relying on a radically different process for light emission, which is independent of the bandgap. Instead of using opposite charge carriers in semiconductors (electrons and holes) at the bottom of their respective conduction and valence bands, which recombine to produce light of frequency $\nu \approx E_g/h$, where E_g is the energy bandgap and h is Planck's constant, QCLs use only one type of charge carrier (electrons) that undergo quantum jumps between energy levels E_n and E_{n-1} to create a laser

photon of frequency $(E_n - E_{n-1})/h$. These energy levels do not exist naturally in the constituent materials of the active region but are artificially created by structuring the active region in ultra-thin layers known as quantum wells of nanometric thickness. The motion of electrons perpendicular to the layer interfaces is quantized and characterized by energy levels whose difference is determined by the thickness of the wells and by the height of the energy barriers separating them. The implication of this new approach, based on decoupling light emission from the bandgap by utilizing instead optical transitions between quantized electronic states, are many and far reaching, amounting to a laser with entirely different operating characteristics from laser diodes and far superior performance and functionality.

2.2. Quantum design

In QCLs, unlike in a laser diode, an electron remains in the conduction band after emitting a laser photon. The electron can therefore easily be recycled by being injected into an adjacent identical active region, where it emits another photon, and so forth. To achieve this cascading emission of photons, active regions are alternated with doped electron injectors and an appropriate bias voltage is applied. The active-region-injector stages of the QC laser give rise to an energy staircase in which photons are emitted at each of the steps. The number of stages typically ranges from 20 to 35 for lasers designed to emit in the 4–8 μm range, but working lasers can have as few as one or as many as 100 stages. This cascade effect is responsible for the very high power that QCLs can attain.

Fig. 1 illustrates a typical energy diagram of two stages of a QCL designed to operate at wavelength $\lambda = 7.5$ μm, which serves to illustrate the key operating principle. The tilt in the conduction band is produced by the applied electric field. Note that each stage comprises an electron injector and active region. The latter contains three quantized states; the laser transition is defined by the energy difference between states 3 and 2, which is determined primarily by the chosen thickness of the two wider wells. A population inversion between levels 3 and 2 is required for laser action. This translates to a requirement that the lifetime of level 3 should be substantially longer than the lifetime of state 2. To achieve that, the lowest level 1 is positioned about an optical phonon energy (~34 meV) below level 2; this ensures that electrons in the latter state rapidly scatter by emission of an optical phonon to energy level 1. Because of its resonant nature, this process is very fast, characterized by a relaxation time of the order of 0.1–0.2 ps. Electrons in level 3 have instead a substantially longer lifetime because of the much larger energy difference between states 3 and 2 so that the electron–phonon scattering process between the latter states is non-resonant. To achieve lasing, however, one must also suppress the unwanted escape route by tunneling from state 3 to states on the right hand side, which form a broad quasi-continuum. Such escape would reduce the level 3 population. To prevent this occurrence, one designs the injector of the next stage as a superlattice with an electronic density of states such that at an energy corresponding to E_3 there is no resonant electronic state, but rather a region of low density of states known as a minigap. Notice instead the dense manifold of states (a miniband) facing levels 2 and 1, which favors efficient electron extraction from the active region. Finally, note that electrons are injected into the upper laser level by a process known as resonant tunneling which ensures highly selective injection when the applied voltage is increased above a certain value. Fig. 1 also shows a transmission electron micrograph of the layer structure of an exemplary QCLs. The dark layers correspond to the AlInAs barrier layers, and the light gray layers to the GaInAs quantum wells.

For wavelengths greater than ~5 μm, the alloy compositions for the wells and barriers are chosen to be lattice matched to the InP substrate, i.e. with the same lattice constant ($Al_{0.48}In_{0.52}As$ and $In_{0.47}Ga_{0.53}As$). The quantum well barrier height for these compositions is the conduction band discontinuity between the two alloys, i.e. $\Delta E_c = 0.52$ eV. For operating wavelengths substantially shorter than 5 μm, the upper laser state moves up in energy so that the barrier for thermal activation of electrons is reduced. In CW operation at room temperature, this process, and a similar one for electrons in the injector regions becomes a limiting factor for the temperature performance (maximum operating temperature and maximum optical power at room temperature or above) because the active region can reach temperatures substantially higher than the laser mount by tens of degrees. This problem is greatly reduced by introducing strained AlInAs/GaInAs heterostructures, i.e. higher Al composition for the barrier and lower In content for the quantum wells. With strain, barrier heights in the 0.7–0.80 eV range can be achieved, which suppresses electron leakage over the barriers. All reported high performance CW room temperature QCLs operating at $\lambda \leqslant 5.2$ μm [6–9,30,31] used such strained heterojunctions. Another critical design parameter to improve temperature performance is the energy separation between the lower state of the laser transition (level 2 in Fig. 1) and the injector ground state.

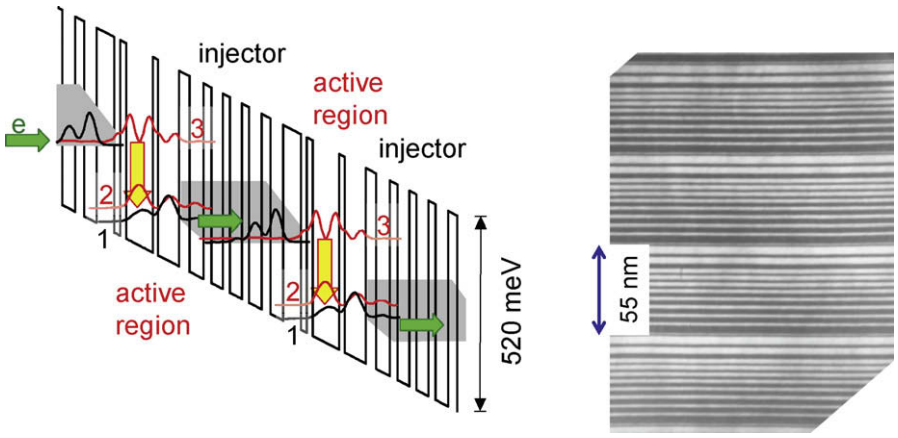

Fig. 1. Left: Energy diagram of a quantum cascade laser emitting at $\lambda = 7.5$ μm. Each stage (injector plus active region) is 55 nm thick. The energy levels and the corresponding probability distributions obtained from solving Schrödinger's equation are shown. The energy well and barriers are made of AlInAs and GaInAs alloys, respectively. Right: Transmission electron microscope picture of a portion of the structure. The white and black contrast regions represent the well and barriers, respectively. For a distributed feedback (DFB) laser, there is a grating on the top surface to select the lasing mode.

It typically should be in excess of 0.1 eV to minimize thermal backfilling of level 2 by electrons in the injector.

In the last few years major improvement in QCL performance (lower threshold and higher power) was achieved by introducing a so-called double phonon resonance design [36]. The active region of this laser has four quantum wells and three energy levels equally separated by the energy of an optical phonon instead of the two levels previously discussed. This active-region design results in a larger population inversion because electrons are more efficiently removed from the lower state of the laser transition.

For a DFB laser, the diffraction grating, which selects a single mode, is either etched on upper surface of the laser ridge or in the material just above the injector-active active region stack on which a cladding layer is subsequently regrown. The period of the grating, d, determines the precise wavelength or laser mode that satisfies the Bragg condition $\lambda = 2n_{\text{eff}}d$, where n_{eff} is the effective refractive index of the waveguide. Light satisfying this condition is strongly reflected off the grating and is selected for laser action. Wavelength tuning in these DFB-QCLs is achieved by increasing the temperature of the laser either with a temperature controller or by using a sawtooth current waveform to drive the laser. Raising the temperature increases n_{eff} and therefore the emission wavelength. Thus, the latter can be positioned in the vicinity of an absorption feature of interest, blue shifted with respect to its peak. A subsequent slow current ramp applied to the QCL can then be used to scan the wavelength across the absorption line as result of Joule heating of the laser active region. Additional modulation of the current by a small signal sine wave of frequency much larger than the ramp can be used to measure the derivative of the spectrum, leading to enhanced sensitivity. Fig. 2 shows the temperature tuning of the emission wavelength of different DFB-QCLs designed to match absorption lines of compounds, which overlap with one of the atmospheric windows. This overlap allows one to achieve high sensitivity (~1 pptv has been achieved in the best case to date) in the detection of trace amounts of these gases in the atmosphere using laser absorption spectroscopy.

3. Broad spectrum quantum cascade lasers

Tunability over a much broader range than what a typical DFB QCL can offer is a highly desirable feature for trace gas analysis, as it enables the parallel detection of multiple chemicals and allows mapping of very broad absorption lines, such as those of liquids. Broad tunability is a necessity for the use of QCLs for the study of transient species such as free radicals and ions, and it is of great utility in the study of the reaction kinetics of free radicals. In this section, we analyze the most effective device design strategies to achieve the goal of broad tunability.

3.1. Broadband single-mode tuning: external cavity grating spectrometer

The key step in achieving broad tunability is the design of a laser with a broad gain spectrum. QCLs, unlike diode lasers, can easily be designed to emit at multiple, and widely differing wavelengths by stacking active regions corresponding to different optical transitions that span a wide range of energies (Fig. 3). Early demonstrations concentrated on dual wavelength lasing [37] followed by a QCL that emitted simultaneously a quasi-continuum of wavelengths between 5 and 8 μm [38]. To ensure quasi-continuous emission, the stages were designed so as to achieve an optimally flat gain spectrum over the emission range of interest. More recently, broadband QCL development has concentrated on continuous single mode tunability over the broadest possible range. In order to achieve that, two design principles have been utilized.

Consider first the aforementioned structure with multi-wavelength stages and a gain per stage engineered to be as broad as possible. This broad gain can be achieved using a so-called bound-to-continuum QCL in which the lower state of the laser transition is a relatively broad continuum consisting of closely spaced sublevels spanning an energy range greater than an optical phonon. The many laser transitions fan out with comparable oscillator strengths, giving rise to a broad spectrum. The application of an external cavity configuration allows selection of the QCL wavelength anywhere within the available QCL spectral gain without changing the chip temperature, thus significantly increasing the laser spectral coverage and allowing much more efficient utilization of the available QCL gain width. This is especially important for the QCL gain media designed to have intrinsically broader gain profiles. Frequency tunability from 961 to 1220 cm^{-1} (24% of the center wavelength) of a pulsed QCL was achieved using a heterogeneous gain medium with a two-wavelength (8.4 and 9.6 μm) active region in a Littrow type EC-QCL configuration [27]. With this laser, single-mode tuning from 1045 to 1246 cm^{-1} was also achieved.

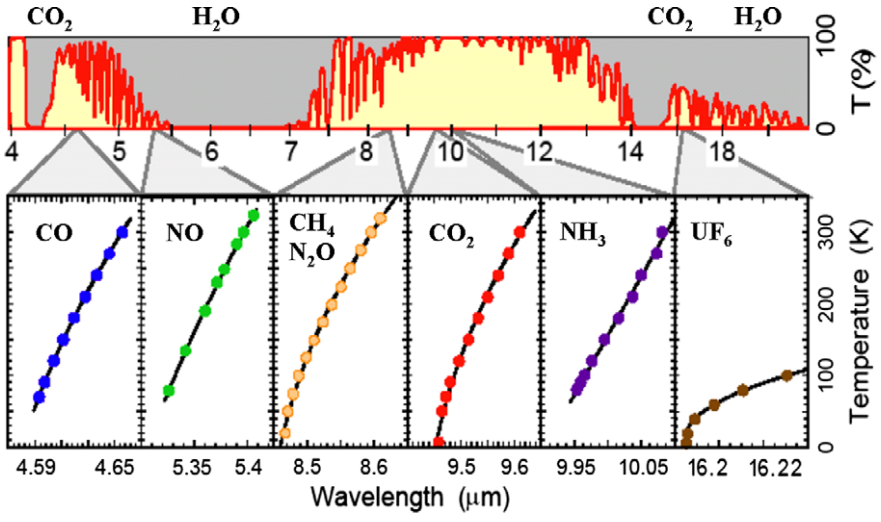

Fig. 2. The upper panel is the transmission spectrum of several hundred meters of air at sea level. Note the two transmission windows below 5 μm and between 8 and 13 μm. The lower panel represents the temperature tuning range of distributed feedback quantum cascade lasers designed to operate in selected regions of the transparency windows where many most common gases have absorption fingerprints. (from Ref. [3] reproduced by permission of IOP).

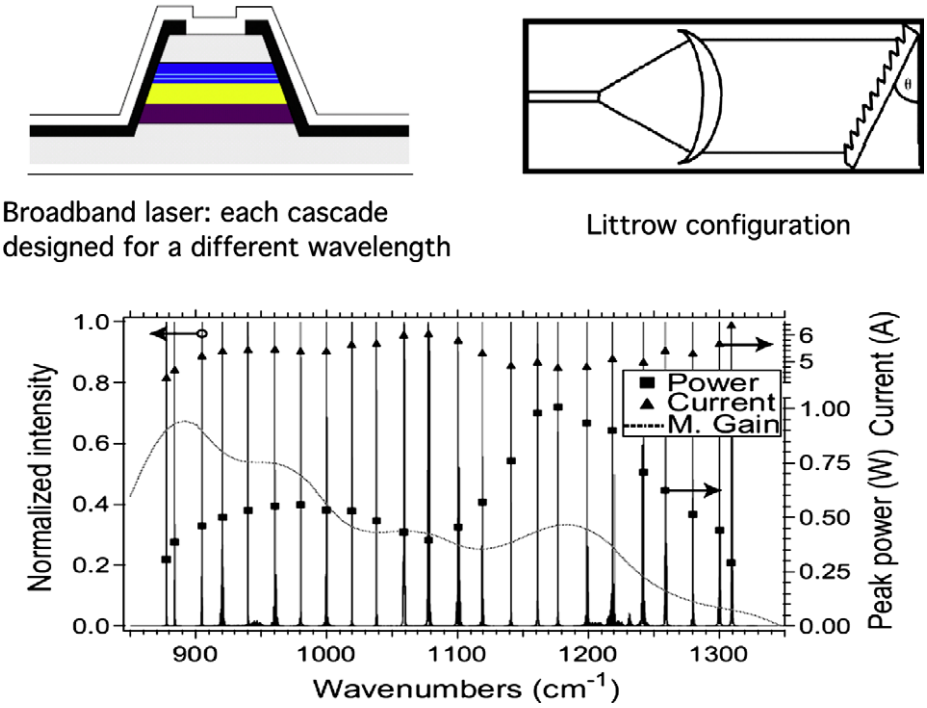

Fig. 3. Broadband quantum cascade lasers. From top left to right, clockwise: Schematics of multicascade configuration; each cascade in general comprises several laser stages (injector plus active region). Schematic of external cavity tuning with grating which provides tuning by change of the angle θ. Demonstration of operation over 432 cm^{-1} [39]. (Reprinted with permission from A Hugi, R Terazzi, Y Bonetti, A Wittmann, M Fischer, M Beck, J Faist, E Gini: Applied Physics Letters 95 (2009) 061103. Copyright 2009, American Institute of Physics.).

Recently [39], lasers using symmetric active-region designs with five different cascades centered at different wavelengths have demonstrated tunability from 7.6 to 11.4 μm with a peak optical output power of 1 W and an average output power of 15 mW at room temperature. With a tuning range of over 432 cm^{-1}, this single mode source covers a continuous emission range of over 39% around the center frequency (Fig. 3). However, the design of a high gain broadband active region covering a significantly larger spectral range without any gaps in the spectral emission is a serious challenge because using more cascades promises even wider tuning ranges, but makes the design more complex.

Typically in an external cavity (EC) laser, coarse wavelength tuning is achieved by rotating the grating, with the feedback needed for lasing arising from the first order grating reflection. However, merely rotating the grating will not result in continuous tuning of the laser over a significant frequency range. Instead the laser frequency will hop from cavity mode to cavity mode. In order to achieve continuous tuning, the cavity length and grating angle must track each other. The situation can be further complicated with a laser with no antireflective (AR) coating by the optical cavity formed by the laser itself. The effects of a laser cavity can be avoided by antireflection coating the facet of the QCL facing the grating to eliminate optical feedback. Several schemes have been devised to track the cavity length with the grating angle [22,24,40].

One reported scheme for wide tuning without mode hops was based on a quantitative coupled mode analysis of the external cavity QC laser [22]. Realizing this tuning scheme involves active and simultaneous adjustment of all three relevant degrees of freedom: grating angle (via precise grating rotation), external cavity length (via PZT controlled optical element), and the optical length of the chip (via driving current and or chip temperature). This tuning scheme utilized a look-up table to identify the correct parametric values of all three variables as a function of the desired wavelength. Another scheme [24] used a somewhat different approach of actively and simultaneously adjusting two degrees of freedom: the QCL chip optical length and the grating angle. A closed loop servo with feedback was used to optimize the cavity length to select and support a desired single mode at every grating angle. In a more recent scheme [40], the grating motion is mechanically constrained to follow a trajectory allowing for the simultaneous tuning of the diffraction grating angle and the laser cavity length, thereby constraining the EC mode to coincide with the wavelength selected by the grating. To avoid problems caused by the laser cavity interaction, a QCL gain chip facet AR coating was developed with sufficiently low reflectivity (<0.001) to suppress the residual etalon effect. A publication describing this design is in preparation. Daylight Solutions Inc. developed this design, and instruments based upon it are commercially available. Fig. 4 shows a spectrum of N_2O obtained with such an instrument.

3.2. Broadband multi-DFB laser spectrometer on a chip

Arrays of DFB-QCLs can be made as single-mode sources covering a wide range of mid-infrared frequencies. For example, a DFB-QCL array has been demonstrated [28], which achieved single-mode lasing coverage of 85 cm^{-1} near 9 μm using a bound-to-continuum active-region design. The devices were fabricated monolithically on the same chip and driven individually by a microelectronic controller. The spacing of the emission wavelengths of the lasers in the array was sufficiently small that for any wavelength within the gain spectrum of the QC laser material, one could select a device in the array and adjust its temperature to produce single-mode emission at the desired frequency. A custom-designed controller was employed, which consisted of pulse generators to power the lasers, direct current bias circuitry to heat individual lasers in the array for temperature tuning, and a serial port interface for computer control of laser firing. Fig. 5 shows the spectra of several liquids obtained with this array. It took approximately 10 s to obtain each spectrum. The results compare

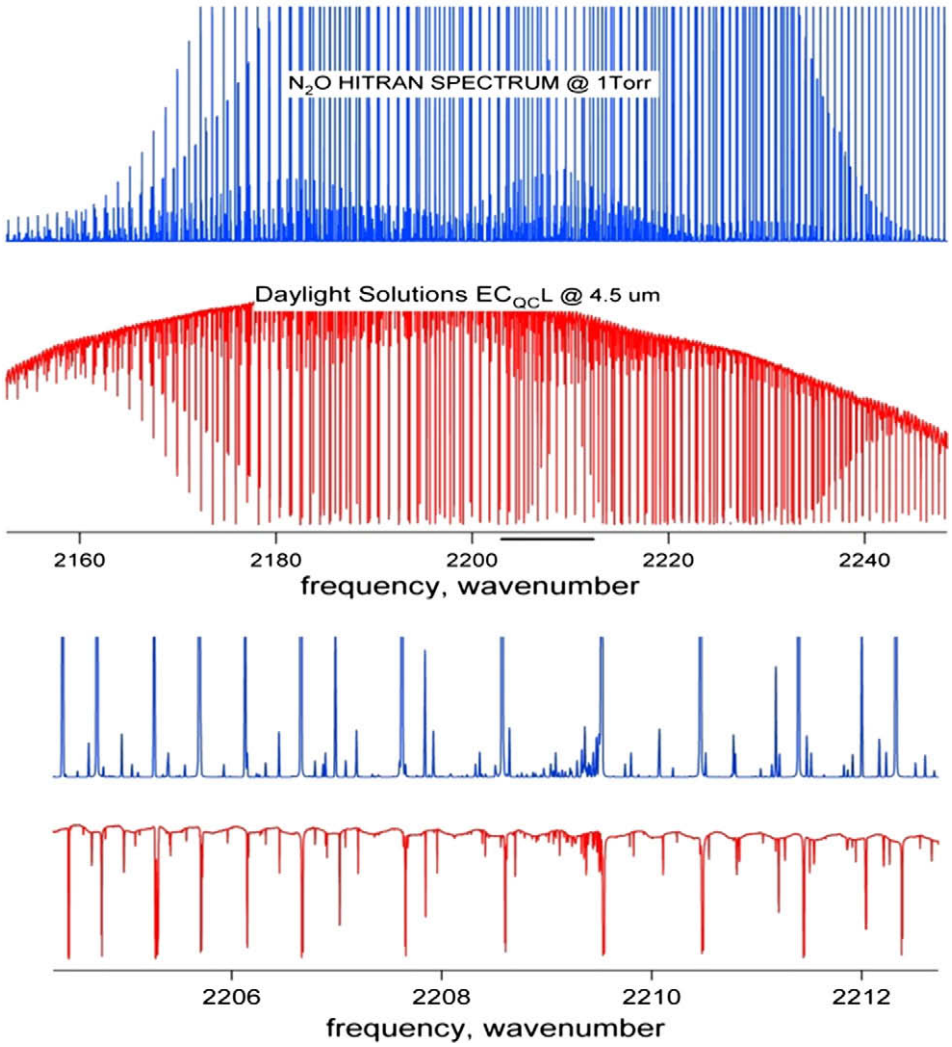

Fig. 4. Absorption spectrum of nitrous oxide at 10 Torr pressure obtained with a single scan of the EC-QCL described in the text. The concentration was kept intentionally high to observe transitions due to low abundance isotopomers. Top two traces: HITRAN simulation and experimental absorption spectrum. Bottom two traces: Frequency axis zoom-in the 2204–2212 wavenumber range (marked with a horizontal bar). (Used by permission of Daylight Solutions).

favorably with spectra obtained using a conventional Fourier transform infrared (FTIR) spectrometer, also shown in Fig. 5.

In order to obtain continuous spectral coverage between the nominal emission frequencies of the individual lasers in the array, one can tune the lasers in a small range with temperature. The lasers can either be heated locally by applying a sub-threshold dc current to tune an individual laser, or the lasers can be heated globally by changing the temperature of the heat sink on which the laser array chip sits. With dc bias current, the tuning was 5 cm^{-1} with 300 mA. Alternatively, the same tuning was achieved by varying the heat sink temperature with a thermoelectric cooler from 252 to 325 K. Local heating using dc current can achieve the desired temperature in milliseconds, while heat sink temperature changes typically take tens of seconds.

We note that the frequency resolution of this QCL spectrometer is determined by the lasers' linewidth, which was measured to be $\sim$0.01 cm^{-1} in pulsed operation and $\sim$0.001 cm^{-1} in continuous-wave operation. This is significantly better than the resolution offered by a typical 'bench top' FTIR ($\sim$0.1 cm^{-1}). Despite the narrower spectral measurement range compared to FTIR spectrometers, we believe that this QCL-based spectrometer can provide a portable alternative to FTIR spectrometers in significant portions of the mid-IR molecular fingerprint region. Most importantly, the fact that it uses lasers instead of a globar (the thermal source used in FTIR spectrometers), has great advantages in terms of much higher brightness, which could be of paramount important in stand-off detection (i.e. the measurement of a spectrum reflected off a surface or aerosol clouds) remote sensing of trace gases. Recently, wavelength beam combining was used to co-propagate the multiple beams from the array of (DFB-QCLs) [41]. The beam-quality product of the array, defined as the product of near-field spot size and far-field divergence for the entire array, was improved by a factor of 21 by using wavelength beam combining. To demonstrate the applicability of wavelength beam combined DFB-QCLs arrays for remote sensing, the absorption spectrum of isopropanol was measured at a distance of 6 m from the laser array [41]. Beam combining was accomplished by a suitably placed grating and transform lens that overlap the beams from each laser in both the near-field and far-field.

In recent work [29] the range of frequencies covered by a single DFB-QC laser spectrometer was greatly increased to cover the available gain spectrum. The emission spectrum of the array (Fig. 6) covers a range of 210 cm^{-1}, much broader than that of the original spectrometer (85 cm^{-1}). Shown is also the spectrum of an individual device indicating its single mode character and a micrograph of the device cross-section.

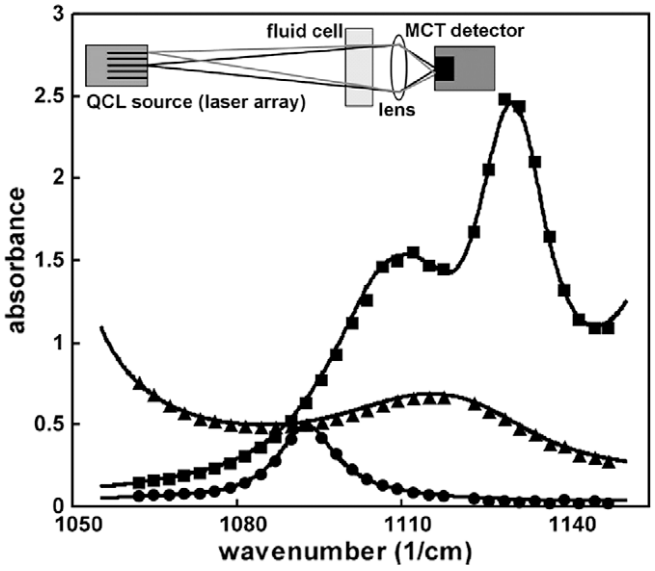

Fig. 5. Absorption spectra of isopropanol (squares), methanol (triangles) and acetone (circles) obtained with an on chip spectrometers consisting of a 32 distributed feedback quantum cascade laser array and with a Bruker Vertex 80v Fourier transform infrared spectrometer (continuous lines). The lasers were operated in a pulsed mode at room temperature [28]. (Used by permission of IEEE Journal of Quantum Electronics). Inset: Experimental setup for mid-infrared spectroscopy of liquids with the quantum cascade laser source.

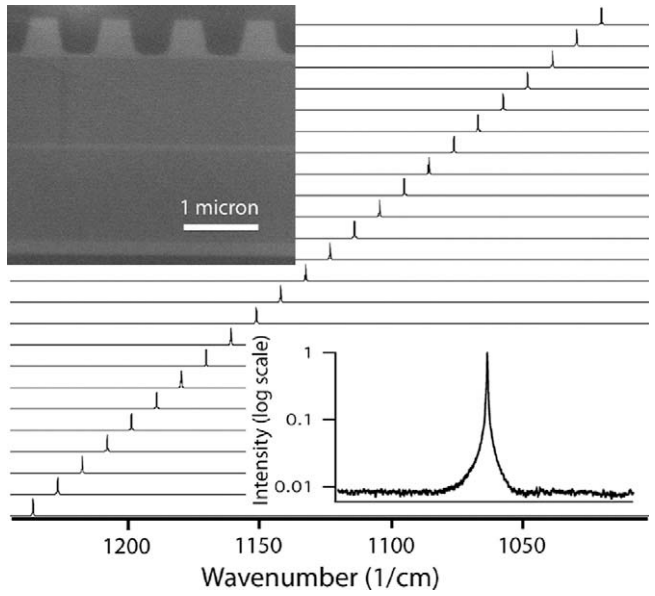

Fig. 6. Spectra of a 24 single-mode DFB quantum cascade laser array [29]. (Used by permission of IEEE Photonics Technology Letters). Laser frequencies are spaced ~9.5 cm apart and span a range of ~220 cm^{-1}. Inset, top left: scanning electron micrograph showing a cross-section of the device, which has been cut along the laser ridge. The grating corrugation can be seen as the rectangular wave near the top of the image, and the two active regions. Designed with gain spectrum maximum at 8.4 and 9.6 μm respectively, are below, with a thin InGaAs spacer between them. Inset, bottom right: Spectrum of a representative laser in the array on a log scale, showing side mode suppression greater than 100. (From Ref. [29] reproduced by permission of IEEE Photonics Technology Letters).

3.3. Quantum cascade laser beam shaping

Semiconductor laser beams, including those of QCLs, usually have a large divergence angle (of around 50°, particularly in the direction normal to the plane of the layers) due to the significant diffraction caused by the thickness of device waveguide which is comparable to the laser wavelength in the semiconductor. Usually the beam collimation is performed using dedicated high numerical aperture aspherical lenses as single element collimators. Other beam-shaping schemes that could greatly reduce QCL beam divergence are important for stand-off detection and remote sensing over long distances, where good collimation is critical. Recently, high beam collimation of QCL was achieved by fabricating integrated collimators directly on laser facets by utilizing surface electromagnetic waves known as surface plasmons. For a review of this and related development in beam engineering of QCLs, see [42].

4. Quantum cascade laser properties and vendors

4.1. Frequency regions for which sources are available

A significant development issue for QCL's has been the problem of achieving short wavelength (high frequency) operation. CW room temperature DFB lasers operating at 2300 cm^{-1} are currently available commercially, as are DFB CW cryogenic temperature lasers operating at 2375 cm^{-1}, but for spectroscopists, the CH stretching region from 3.7 to 3 μm (2700 to 3300 cm^{-1}) is perhaps of greatest interest. The upper frequency limit of QCLs is determined by the maximum barrier heights defining the quantum wells. Reaching wavelengths below 4 μm has proven to be very challenging [17,43–48]. However this situation may soon change, as research in this field is active in several groups [45–47,49–54]. In the most widely used AlInAs/GaInAs material system, a short-wavelength mid-infrared QCL, emitting pulsed at 3.5 μm (at 280 K), was demonstrated using strain-compensated AlInAs/GaInAs on InP substrates [43]. Shorter wavelengths down to 3.0 μm are possible but at a cost of substantially lower temperatures. Several very recent breakthroughs in pulsed room temperature operation toward 3 μm have been described based on using heterostructures with very high conduction band offsets: InAs–AlSb on InAs substrates [49] and InGaAs–AlAs(Sb) on InP substrates [45,54]. In [49] QCLs emitting at a wavelength near 3.3 μm up to a temperature of 400 K in pulsed mode were reported. Recently, a pulsed room temperature single mode operation DFB QCL at a wavelength as short as 3.34 μm (~3000 cm^{-1}) with an output power of 0.8 W has been demonstrated [51]. QCLs emitting at wavelengths near $\lambda = 3.1$ μm (~3225 cm^{-1}) at room temperature have been demonstrated [54]. The lasers operated in pulsed mode with an optical power of 8 mW at 295 K. By cooling to cryogenic temperatures wavelengths as short as 2.75 μm (~3600 cm^{-1}) have been demonstrated [45].

In the 3–4 μm spectral region, there is another technology that has demonstrated significant performance improvements, the interband cascade laser. The concept was pioneered by Yang in 1995 [55] and is based on an interband optical transition between the valence band of GaSb and the conduction band of an adjacent InAs layer, separated from the GaSb by a thin AlSb tunnel barrier. What makes this optical transition possible is the broken gap band-alignment of the GaSb/InAs heterojunction, whereby the top of the valence band of the former is above the conduction band bottom of the latter. This band arrangement permits cascading of many identical stages, just as in QCLs, that an electron can sequentially tunnel through multiples stages emitting a laser photon at each stage thus increasing the optical power. The best result reported so far with this technology is CW operation at 300 K for a $\lambda = 3.75$ μm device with an optical power in excess of 10 mW [56].

Concerning lower frequency operation, as QCL operation moves further into the mid-infrared region-well past the 8–13 μm transmission window of the atmosphere one encounters phenomena which exclude laser action in a certain frequency window. To understand that, let us note that in all polar semiconductors, and

in particular, for the III–V semiconductors used in QCLs, light of frequency within the narrow band defined by the longitudinal and transverse optical phonon frequencies suffers strong reflection when normal-incident on a semiconductor surface. This band is known as 'Restrahlen', a German word meaning 'residual rays'. Light in the Restrahlen band cannot propagate in the medium, and is reflected back due to the formation of coupled photon–phonon modes (known as polaritons) made possible by the polar nature of chemical bonds in III–V semiconductors. Approaching this region from higher frequencies, one also encounters multiphonon absorption, which combined with the Restrahlen effect, is responsible for the gap in QCL frequency coverage in the range between about 200 and 400 cm^{-1}. Approaching this region, QCL performance deteriorates. So far, approaching this region from the high frequency side, the longest wavelength operation achieved [57] is 24 μm (417 cm^{-1}) in pulsed operation at cryogenic temperatures. However, if the challenges of making QCLs based on Si/Ge alloys can be overcome, uninterrupted wavelength coverage from the mid-IR to the far-IR will become possible because there is no Restrahlen band in SiGe due the non-polar nature of the bonds.

The region below the Restrahlen frequency band extending between approximately 30 and 300 μm is usually denoted as Terahertz in the current literature. Because adequate sources in the THz region are difficult to access, there is considerable activity in developing THz QCLs. For a recent reviews of this field see Refs. [33,58]. The low frequency limit of QCLs is around 1 THz (33 cm^{-1}) but it requires a magnetic field. The first THz QCL, operating at $\lambda \sim 85$ μm (3.5 THz) was reported in 2002, but despite serious efforts by a number of groups, room temperature operation seems blocked. The current highest operating temperature is 186 K [59]. Lasing at 245 K has been achieved [60], but this required placing the device in a high magnetic field.

An alternative QC laser approach to THz generation is the difference frequency mixing inside a mid-IR laser operating simultaneously at two different frequencies. At present the best output power by QC DFG is about 7 μW at 80 K and 300 nW at room temperature [61]. However, the DFG THz frequency spectrum was not sharp. It is estimated that device optimization should lead to power levels ~1 mW at room temperature.

4.2. Laser operation

Some spectroscopic applications, such as trace gas monitoring or atomic line experiments, require only modest frequency tuning of perhaps 5 cm^{-1}. For these cases, the optimum solution is a DFB QCL, provided that one can be obtained that works in the desired frequency region.

The operation of DFB QCL is simple. In addition to the laser, a thermoelectric temperature-controlled mount and high current stability DC power supply capable of delivering about 1 A at 10 V are required. As the current passing through a QCL is increased, the device will reach a threshold where the gain due to population inversion equals the optical losses and lasing begins. Output power will increase, and then level off and decrease. Generally in CW operation, output power is limited by the active region temperature rise or the extrinsic carrier density in the injector regions, which needs to be sufficiently large to allow injection of a high current, but not too high, so as to avoid excessive optical losses by free carrier absorption. In pulsed low duty cycle operation, the active region is at the laser heat sink temperature and at room temperature the maximum peak output power is limited by the energy misalignment between the upper state of the laser transition and the injector at high enough currents. At a given heat sink temperature, more peak power can be obtained in pulsed operation at low duty cycle.

As already mentioned, frequency tuning of a DFB QCL is performed by thermal tuning of the refractive index. Because QCLs are so tiny and thus have quite small heat capacities, their temperature can be changed rapidly by modulating the operating current. Thus wavelength modulation over a Doppler-broadened line at a few tens of kHz is simple.

For many spectroscopic applications, the tuning range of a DFB QCL is inadequate. As discussed above, the most elegant way to achieve broad tuning is to gang multiple DFB-QCLs into an array [28,29]. These provide a very compact broadly tunable mid-IR source. However, development of these laser arrays is at a very early stage. The device requires optics to combine the lasers into a single beam, which can be achieved using a grating and lens [41]. As also previously discussed, the alternative is to incorporate a QCL with a broad gain spectrum [27,38,62–64] into an external cavity [22–26,40,65,66]. However, scanning without mode hops requires using controllers to track cavity length and grating angle.

4.3. Noise and linewidth of quantum cascade lasers

The intrinsic noise of QCLs has been explored both in theory [67–71] and by experiment [67,72–75]. The focus of these studies has been on high frequency noise at 10 MHz and above, up to GHz. For most spectroscopic applications, the detected signal is in the kHz range or below where $1/f$ noise is expected to dominate. We have been able to find no reports in the literature of systematic exploration of noise below 1 MHz. This is not surprising because this noise in most situations is primarily determined by the quality of the current source for the QCL and is thus not readily transferable from one instrument to another.

So far we have discussed amplitude noise. The other aspect is frequency noise. Recently, the work of Paolo De Natale's group at the European Laboratory for Nonlinear Spectroscopy has been brought to our attention [76]. They measured the frequency noise power spectral density of a free running mid-IR (λ = 4.33 μm) single mode cryogenically cooled QCL using the side of a Doppler broadened molecular transition of CO_2. This well-established method allows one to convert laser frequency fluctuations into detectable intensity variations with negligible added noise [77]. The spectrum of the intensity transmitted by this discriminator, when the laser frequency is locked to the half height position i.e. where the small signal response is linear, reproduces the spectrum of the laser frequency fluctuations 'amplified' by the slope of the absorption profile. The signal was detected with a fast 200 MHz bandwidth HgCdTe detector. For these measurements, an ultra-low noise current driver approaching shot noise was developed, thus enabling the measurement of the intrinsic laser noise. Between 10 and 100 MHz, a white noise plateau is observed, which decreases with increasing drive current-to-threshold-current-ratio (I/I_{th}) and corresponds to an intrinsic QCL linewidth of 510 Hz for I/I_{th} = 1.54 and a CW optical power of 6 mW.

The observed hyperbolic dependence on I/I_{th} is in qualitative agreement with recent theoretical predictions of the QCL linewidth. For I/I_{th} = 1.54 its value is about 20% larger than the measured valued, a discrepancy that could be in part explained from uncertainties in the active region parameters used in the calculation such as lifetimes and upper laser level injection efficiency [78]. The latter had been previously assumed to be governed by the standard Schawlow–Townes formula of laser theory, augmented by the factor $(1 + \alpha^2)$, where α is the alpha parameter which accounts for the effect of refractive index variations caused by electron density fluctuations. In QCLs, however, these variations are negligible at the peak of the gain spectrum because the latter is in most cases symmetric (Lorentzian). This fact led the authors of [1] to predict that α in QCLs should be very small. Several subsequent measurements confirmed that [79–82]. The remarkable feature of Yamanishi et al. [78] is that it

predicts, for small α, linewidths even narrower than the Schawlow–Townes (Δ_{ST}) value by a factor depending on I/I_{th} and on the ratio of the spontaneous emission rate coupled into the laser mode to the total relaxation rate of the upper level. In most lasers, the latter is dominated by spontaneous emission, which is the fundamental source of noise. The fact that, in QCLs, the non-radiative relaxation rate from the upper level is instead many orders of magnitude larger than the spontaneous rate from the same level leads to the reduction of the laser linewidth well below the Schawlow–Townes limit [78]. Note that in the above experiments the measured QCL linewidth is substantially below the calculated linewidth (4 kHz at a laser power of 6 mW) using the Schawlow–Townes formula.

4.4. Sources of QC lasers

There are several QCL wafer providers and commercial manufacturers of QCLs and ICLs as well as several companies that have developed laser systems incorporating QCLs. These are listed in Table 1.

5. Spectroscopy with quantum cascade lasers

Because of their broad gain profiles, relatively high power, and narrow line widths, QCLs will be useful in a wide variety of spectroscopic experiments and applications. They have the additional advantages of being extremely compact, with a volume of much less than a cubic centimeter, operating at room temperature, and having long lifetimes. It should be possible to manufacture them relatively cheaply, since the material system (InGaAs/AlInAs) is commonly used for optoelectronic and high speed electronics applications at communication wavelengths and is epitaxially grown on InP using the same commercial MBE and MOCVD InP based growth platforms widely employed in III–V semiconductor device production. In addition, QCL device processing is basically very similar to that of well established and mass produced DFB telecommunication laser technology in near-infrared spectral region. QCL research and development continues to be an extremely active field so that we can expect new and better QCLs in the near future.

Because the early QCLs had tuning ranges of only a few wavenumbers, almost all of the early use of them was in trace gas monitoring of small molecules with well resolved rotational structure. All that was required was a laser that could be tuned to a line of the gas of interest that did not overlap a line of another substance present in the sample. Since most analytical applications were monitoring of trace gases in the atmosphere, this meant that normally only overlap with lines of water and carbon dioxide had to be avoided. Excellent selectivity for a particular molecule without loss of sensitivity was possible because as long as the width of a rovibrational line was determined by pressure broadening, a reduction in the total pressure by pumping analyte away did not reduce its peak absorption. This enhanced selectivity has led to an emphasis on point sampling methods in contrast open path absorption, because the pressure of a sample could be reduced, thereby narrowing absorption linewidths by more than an order of magnitude and improving selectivity without significant reduction in peak absorption or sensitivity.

Early QCLs output powers of more than a milliwatt were sufficient for a number of improvements in conventional absorption spectroscopy. If the light source is weak, there is an optimum path-length for a multi-pass system because light attenuation by multiple reflections soon makes detector noise limiting. One milliwatt of laser power is typically a factor of 10 million greater than the noise of the best detectors, making many reflections possible. Before QCLs became available, Aerodyne Research Inc. had been active in developing relatively compact astigmatic long pass multiple reflection cells, which match well the typically more powerful QC sources.

More IR power also enabled more feasible cavity-enhanced spectroscopies. While it is true that with a perfectly mode-matched monochromatic input to a cavity, the light can pass through a cavity unattenuated, even approaching such perfection is challenging, and is unnecessary with enough power.

As available QCL power continues to rise, QCLs are finding more application to photoacoustic spectroscopy, where the signal-to-noise ratio is initially clearly limited by source power. Eventually as the power rises, the noise floor will be determined by unwanted excitation of the sound detector(s) by the light exciting vibrations in the cell windows or by scattered light exciting vibrations of cell walls. Through careful design, this limit can be pushed back to accommodate watts of laser power. Thus, as QCLs continue to become more powerful, photoacoustic spectroscopy will become an even more important tool for high sensitivity spectroscopy. Ultra-compact high sensitivity trace gas monitors can be created by combining QCLs with quartz tuning forks to perform quartz-enhanced photoacoustic spectroscopy (QEPAS) [83]. In this approach, the laser beam is focused between the two tines of a quartz tuning fork, such as those used in wristwatches.

6. Examples

6.1. Long pass absorption

Combining mid-infrared QCLs with the techniques of long path-length absorption spectroscopy provides a flexible and

Table 1
List of companies providing QCL wafers, QCL sources and sensor systems.

Company name	Company website	QCL wafers	QCL sources	QCL systems
AdTech Optics Inc.	www.atoptics.com	X	X	
Aerodyne Research Inc.	www.aerodyne.com			X
Alcatel-Thales III-V Lab	www.3-5lab.fr		X	
Alpes Lasers	www.alpeslasers.ch		X	
Archcom Technology Inc.	www.archcomtech.com	X		
Cascade Technologies	www.ctscientific.com		X	X
Daylight Solutions Inc.	www.daylightsolutions.com			X
Hamamatsu	www.hamamatsu.com		X	
IQE	www.iqep.com	X		
Laser Components Inc.	www.lasercomponents.com		X	
Maxion Technologies Inc./PSI (Physical Sciences Inc.)	www.maxion.com	X	X	
Nanoplus Inc.	www.nanoplus.com		X	
Neoplas Control Inc.	www.neoplas-control.de			X
nLIGHT Corporation	www.nlight.net	X		
Pranalytica Inc.	www.pranalytica.com		X	X
QuantaRed Technologies	www.quantared.com			X
Spire Corporation	www.spirecorp.com	X		

straightforward route to high sensitivity and high precision measurements of a wide variety of gas phase molecules. Increasing the absorption path-length is a universal method of increasing the absorption depth and thus the sensitivity of spectroscopic measurements. For strongly absorbing gases at high concentrations, a few millimeters of path may be sufficient, but some measurement problems require a path-length of hundreds of meters. As mentioned earlier, low pressure (typically ~1/20 atmosphere) yields narrow absorption lines for maximum sensitivity and minimum interference from other gases. The long path-length generally is provided by a multi-pass cell, an optical device to fold the path into a compact volume. Popular types of multi-pass cell include the White cell [84], Herriott cell [85] and astigmatic Herriott cell [86]. In this section, we present recent examples of using QCL's with long path-length multi-pass cells for high sensitivity and high precision measurements in atmospheric research.

The basic configuration of a long path-length spectrometer is quite simple, comprising a laser, followed by a multi-pass cell and then a detector. A cartoon of such a configuration is shown in Fig. 7. The multi-pass cell has a definite path-length, and a considerable fraction of the laser light may be transmitted to the detector, minimizing the effects of detector noise. The basic measurement of the absorption involves a comparison of three quantities, the signal at zero light, the signal due to background light (on either side of the absorption) and the light signal centered on the absorption line. Ideally, one should measure the area of the absorption line, i.e. the integrated deviation of the light signal from background, but this is rarely done with laser sources because very high S/N and a flat baseline is required to separate the slowly decaying wings due to pressure broadening from the baseline. Instead the absorption lineshape is fit with a Voigt function. To measure the absorption line, the laser may be linearly scanned over the line to observe the direct absorption shape, or it may be modulated sinusoidally to produce signals that are analyzed in terms of harmonic content. Either method can yield low noise measurements, as long as the sweep or modulation frequency is high enough to avoid low-frequency laser flicker noise. The limiting noise source may be detector noise (with low optical power) or noise associated with the light, such as laser noise or fluctuations of optical interference fringes produced in the multi-pass cell.

In practice, the configuration of a long path-length spectrometer tends be more complicated than that shown in Fig. 7. For example, two or more lasers may be combined to pass through the cell in order to measure multiple substances. A single detector may be used if the lasers are time multiplexed. A fraction of the laser output may be split from the main beam for diagnostic or control purposes. Monitoring the laser output power allows one to reduce the effects of power variations with normalization. If a fraction of the laser output passes through a short cell containing a high concentration of the gas of interest, the laser frequency may be locked to a specific absorption line.

The laser spectrometer shown in Fig. 8 is part of an instrument suite developed at Harvard University and Aerodyne Research Inc. [87–89]. This particular instrument has two pulsed, thermoelectrically cooled QCLs, one operating at 7.8 μm to measure CH_4 and N_2O

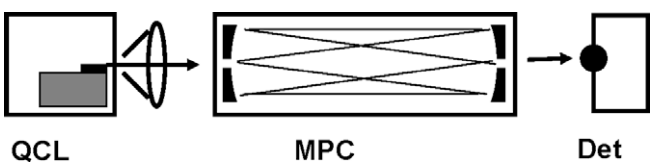

Fig. 7. Schematic diagram of a very simple spectrometer with a single quantum cascade laser, a multi-pass cell (MPC) and a detector (Det). The QCL is mounted on a thermoelectric cooler in a hermetic enclosure, and a lens or other optical element is used to collect the widely divergent light into a narrow beam.

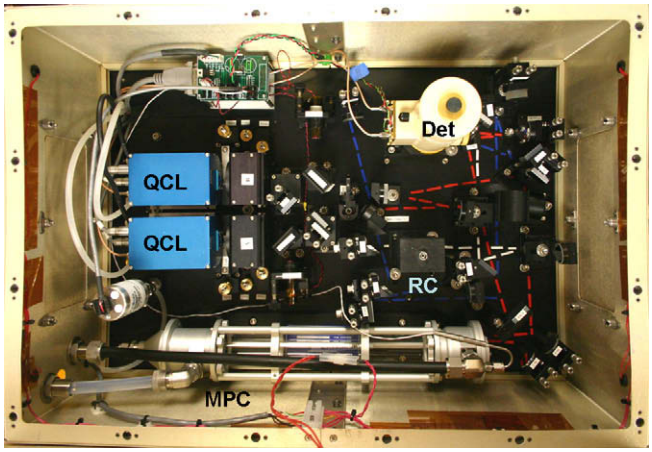

Fig. 8. Photograph of a dual quantum cascade laser spectrometer used for atmospheric research. The pulsed QCLs are in blue housings. Beams from the two lasers are combined to pass through a multi-pass sample cell (MPC) with 76 m path-length. A small fraction of the combined beam is split off to go through a short reference cell (RC). Another split-off path is used for power normalization. All three optical paths end at a pair of liquid nitrogen cooled detectors in a single dewar (Det).

and another at 4.6 μm to measure CO. The lasers are rapidly swept across the spectral lines, and measured spectra are synchronously co-added then fit with computed spectral forms based on the high resolution spectral parameters tabulated in the HITRAN database [90] to derive concentrations.

The (astigmatic Herriott) multi-pass absorption cell [86] in this instrument has 76 m of path in a volume of 0.5 l. The detectors in this instrument are liquid nitrogen cooled for maximum performance. The demonstrated sensitivity at 1 Hz is 0.2 ppb for CO (ambient concentrations vary widely), 0.8 ppb for CH_4 (1 part in 3000 of ambient) and 0.1 ppb for N_2O (also 1 part in 3000 of ambient).

The dual QCL spectrometer described above has been integrated into an instrument suite aboard NASA's Hiaper research aircraft, and already has flown on one mission sampling the atmosphere (nearly) from pole to pole. The Harvard University (Steve Wofsy group) instrument suite also contains a second QCL instrument for measuring CO_2. For the CO_2 instrument, a precision of 1 part in 10 000 of ambient (30 ppb in 1 s) is achieved with only ~15 cm absorption path-length. The recently completed first sampling mission, with the code name 'HIPPO', for 'Hiaper Pole to Pole Observations of carbon cycle and greenhouse gases', has produced the most comprehensive profile of a suite of greenhouse gases from the boundary layer to the lower stratosphere and from the south Pacific to the high Arctic [91]. Continuing HIPPO flights will help to constrain global models of greenhouse gas sources, sinks and transport.

The Hiaper QCL instruments illustrate an important distinction in atmospheric measurements, the need in some cases for high precision versus high sensitivity. In a high precision measurement, one needs to distinguish small changes in a nearly constant gas concentration. In a high sensitivity measurement, one seeks to quantify a gas with very low (and perhaps highly variable) concentration and its quantitative detection is the object. High sensitivity (but not necessarily high precision) is required for reactive gases and radicals which are present at very low and variable levels. In such cases, a detection limit in the pptv range may be needed, but one would not expect that measuring changes of 0.1% would be useful. High precision is needed for stable gases, such as N_2O, where sources and sinks are revealed by very small fractional changes in concentration. For N_2O, measuring changes of 0.1% of the ambient level of ~325 ppbv can be highly significant. In

common with high sensitivity measurements, high precision requires low detector and laser noise, and low interference from other substances. Distinct from high sensitivity measurements, high precision requires stable scale-factor, high degree of linearity and low noise associated with the nominal concentration. Another challenging atmospheric measurement problem that requires high precision is isotopic analysis, and QCL-based spectrometers have recently been developed that meet the challenge. For the ratio of $^{13}CO_2$ to $^{12}CO_2$, both isotopologues must be measured with a precision on the order of 10^{-4} to be useful in answering environmental questions. A CO_2 isotopic analysis spectrometer using a pulsed QCL operating at 2310 cm^{-1} has been developed at Aerodyne Research Inc., in collaboration with EMPA, the Swiss Federal Laboratories for Materials, Testing and Research [92,93]. This instrument measures three isotopologues ($^{12}CO_2$, $^{13}CO_2$ and $^{12}C^{18}O^{16}O$) at ambient concentrations, with a precision for each of $\sim 10^{-4}$ in 1 s, and can operate in field settings. The capacity for continuous field measurement of isotopic ratios of atmospheric gases opens up new possibilities in atmospheric research.

Field applications of QCL-based instruments have been greatly facilitated by the recent availability of thermoelectrically (TE) cooled mid-infrared detectors. When liquid nitrogen (LN_2) cooled detectors are no longer needed, fully cryogen free mid-IR instruments can be used for long term in situ air monitoring. While currently available TE cooled IR detectors have higher noise than LN_2 cooled detectors, the higher power of new QCL's reduces the need for high detector sensitivity making the use of TE cooled detectors suitable for many applications. A fully non-cyrogenic pulsed QCL CO_2 isotopic spectrometer has operated continuously for months in a research station on the Jungfraujoch, also considered to be the highest railway station in Europe. The precision achieved with that instrument is almost as good as in similar instruments with LN_2 cooled detectors.

As a final example of high precision in long path spectroscopy, we describe recent results with a completely non-cryogenic instrument using a CW QCL and a 210 m path-length cell measuring isotope ratios of methane in ambient air in a field experiment. These results thus combine several aspects of recent developments in QCL-based long path-length spectroscopy. The ambient concentration of methane ($\sim$1800 ppb) is only $\sim$0.005 times that of CO_2, so measuring $^{13}CH_4/^{12}CH_4$ with useful precision is a challenge. A QCL based spectrometer for methane isotopologues has been developed at Aerodyne Research Inc., in collaboration with the Wofsy group at Harvard University. That instrument has shown a precision in $^{13}CH_4/^{12}CH_4$ of 1.3‰ (per mil) in 1 s and 0.2‰ in 100 s, which is a useful level of precision for environmental studies. This instrument can measure changes in fractional absorption as small as 7×10^{-7} with 100 s averaging. This instrument has been measuring isotopic ratios of ambient methane at a fen in New Hampshire since mid-summer, 2009.

Several examples have been presented where QCL's have been used in long path-length spectroscopic instruments for atmospheric research, and where concentration measurements have been demonstrated at high levels of precision. Numerous such QCL-based instruments are currently in use in field settings, helping to answer pressing questions in atmospheric and environmental research. New types of mid-IR QCL based instrumentation are continuously under development, including some with exceedingly long effective path-lengths. The performance demonstrated by relatively simple long path-length absorption instruments has helped to set a standard to which novel methods may be compared.

6.2. Cavity methods

Instead of using multi-pass cells, another way to obtain a very long path-length is through application of resonant optical cavities. Cavity ringdown spectroscopy (CRDS) [94–97] is intrinsically background-free. When carried out with high power pulsed lasers, it is very simple to implement, requiring in addition to the laser, only high quality cavity mirrors, a reasonably fast detector and suitable data acquisition. However, this technique is harder to implement with QCLs, which have maximum pulse powers only a few times their CW output. Nevertheless, such a technique has been demonstrated [98]. At the cost of additional complexity, this power limitation can be overcome by locking the cavity to the laser to fill the cavity followed by rapid laser turn off. Alternatively, the cavity can be dithered while a CW laser is scanned slowly [99,100]. All of these approaches were hindered by short ringdown times: high reflectivity mirrors in the mid-infrared so far do not have the remarkably high reflectivity of near-IR mirrors. Since the cavity ring-down time is proportional to the mirror separation and inversely proportional to the mirror loss, either the mirror separation must be increased or the relative precision of measurement of ring-down time improved in order to obtain the same low minimum detectable absorption coefficients found in the near-IR. Nevertheless there have been several applications combining CRDS with QCLs.

A more popular method has been the direct measurement of light absorption by the sample in the cavity. In order to obviate a requirement that the cavity and laser be locked together, the most common approach has been to use off-axis integrated cavity output spectroscopy (OA-ICOS) [101–104]. This method is very closely related to absorption spectroscopy using a multi-pass cell with the principal difference being that in ICOS the beams are allowed to overlap on the mirrors after many passes through the cavity. In this approach, by using fairly large mirrors and introducing the laser beam off the cavity axis, high order cavity modes are excited. The principal effect limiting sensitivity is output fluctuations (noise) caused by transmission noise due to the resonant mode structure. One approach for minimizing this noise is to arrange that the laser spots on the mirrors exhibit a circular pattern similar to those of Herriot multi-pass cell. If many passes of the cavity take place before any of these spots overlap, interference effects are minimal because the path-length before overlap exceeds the coherence length of the laser. By introducing a small amount of astigmatism, the entire surface of the mirrors can be used [105]. Another approach for removing mode noise in OA-ICOS is to vibrate the mirrors [101–103]. This causes many mode hops to take place within the time required to empty the cavity, effectively averaging out this noise. Thus the trade-off between multi-pass absorption and ICOS is that in multi-pass absorption, this mode noise is not present because the spots never overlap, but for similar mirror size and separation, the total path-length can be much greater in ICOS. Since there are no transparent holes in the mirrors in ICOS to admit and allow the exit of the beam, ICOS requires more laser power, which is available with QCLs. A practical medical application of QC laser OA-ICOS is the measurement [106] of NO and CO_2 in the breath. More recently, Anderson's group at Harvard has constructed [107] an OA-ICOS instrument for measurement of isotope ratios in water in order to obtain information about the role of water in global climate change.

6.3. Photoacoustic spectroscopy

Laser photoacoustic spectroscopy (PAS) is a powerful technique for trace-level gas sensing because it combines high sensitivity and the ruggedness required for field deployable instrumentation [108,109]. With a room temperature laser source, a PA based analyzer does not require cooling of any of its components, features high linearity and dynamic range and is virtually background-free, i.e. power normalized PA signal is proportional to the absorption coefficient of a measured sample. Room temperature external cav-

ity quantum cascade lasers (EC-QCL) are a perfect match for the PAS technique because of their narrow linewidth, high output optical power, room temperature operation and continuous tunability. The results reported below were obtained by an R&D group (including author M.P.) at Pranalytica Inc. (Santa Monica, CA). A detailed account can be found in Refs. [24,25]. All figures below are reproduced with minor changes from the same Refs. [24,25].

In a typical PAS setup [108] the laser source is directed through a photoacoustic cell. Upon exiting the cell, the laser beam is directed to a power meter. The photoacoustic signal due to laser radiation absorption by the molecule of interest is measured via a microphone. The cell is closed with AR coated entrance and exit windows and gas sample is introduced through inlet and outlet ports. The PAS cell cavity is designed to be an open pipe acoustical resonator and the laser beam is amplitude-modulated at the frequency of the first longitudinal resonance of the resonator; in the present implementation, this is ~1800 Hz. The microphone output signal is amplified and sent to a lock-in amplifier. The ratio of the lock-in amplifier output and the laser power measured by the power meter is proportional to the absorption coefficient of the analyzed gas. When the PAS cell is properly vibrationally isolated, the resonant nature of the PAS cell enhances the PAS signal by the quality factor of the resonance, improving the signal-to-noise of the gas signal.

6.3.1. Spectroscopy of nitrogen dioxide

NO_2 is a smog and particulate matter precursor and one of the routinely monitored pollutants [110]. Ambient concentrations of NO_2 typically are from 5 to 20 ppb levels. Ambient NO_2 sensing at 6.2 μm is often complicated by potential interference from water vapor. To demonstrate sensor performance in realistic conditions, the spectra were recorded [25] both in clean dry air (CDA) and in air with added 0.85% absolute humidity (corresponding to 28% relative humidity at 25 °C). PAS spectra of water vapor and NO_2 in humidified air, recorded in the spectral range around 1600 cm^{-1}, are shown in Fig. 9 along with the HITRAN molecular absorption database [90] (www.HITRAN.com) simulations.

A triplet spectral feature of NO_2 (labeled A in Fig. 9), centered at 1599.95 cm^{-1} and seen to be water-interference free, was used to evaluate the PAS sensitivity for detecting NO_2.

Fig. 10 shows PAS response linearity for several NO_2 concentrations from 10.4 ppm to 100 ppb. The background noise level is equivalent to 0.5 ppb of NO_2 (S/N = 1) and arises predominantly from the electrical noise of the cell microphone preamplifier and not from the laser background (Fig. 10).

6.3.2. Spectroscopy of trinitrotoluene (TNT) vapor

An FTIR spectrum of TNT vapor reveals two broad strong absorptions in the 6–8 μm region [111]. The peak at 7.4 μm was selected for TNT sensing based on availability of 7.3 μm center gain media and the EC-QCL analyzer described above. A TNT gas phase sample was created by entraining headspace vapor of a solid sample of TNT8 into the controlled flow of dry air. The temperature of the TNT sample was controlled and varied from room temperature to 60 °C. The gas transport lines from the TNT sample chamber to the PAS cell and the cell itself were maintained at 60 °C to prevent condensation of TNT vapors on the walls.

The left hand graph on Fig. 11 shows a PAS spectrum obtained when the TNT sample was kept at 24, 35, 45 and 55 °C, respectively [24]. A number of sharp absorption features arising from residual water vapor in the system (as verified using water vapor absorption spectra obtained from HITRAN simulations) occur at certain wavelengths in the same region of wavelengths. The QCL-PAS spectrum, though it qualitatively matches the FTIR spectrum, is significantly broader than the FTIR. In fact, the QCL-PAS spectrum appears to consist of two distinct features, one centered at

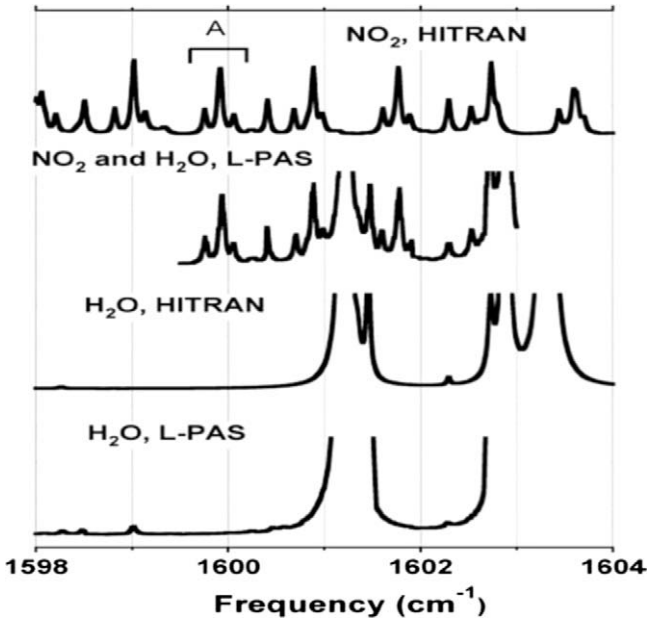

Fig. 9. HITRAN and PAS spectra of water and nitrogen dioxide. (From Ref. [25] Copyright PNAS 2006).

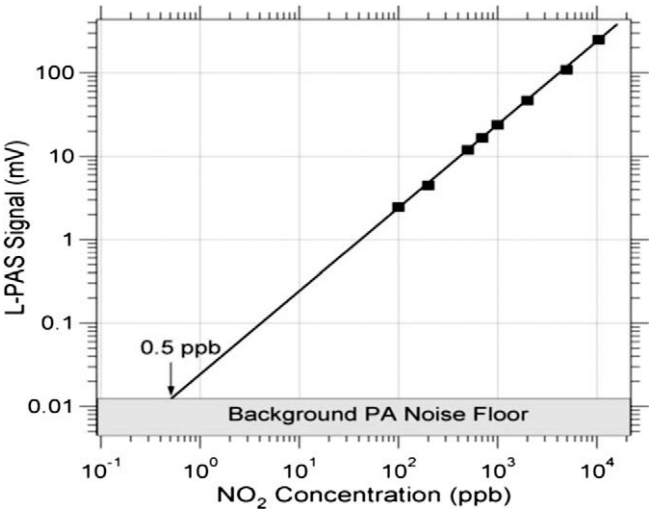

Fig. 10. NO_2 signal versus NO_2 concentration showing the linearity of the system response. The detection limit is determined by the concentration at which the signal equals the noise of the PA system. (From Ref. [25] Copyright PNAS 2006).

~7380 nm matching the expected absorption feature of TNT and the second one centered at ~7300 nm that arises from an unknown impurity in the commercial grade TNT. The unknown impurity gradually disappeared as the TNT sample was kept at 100 °C for 48 h while flushing the sample with clean dry air. The right hand graph of Fig. 11 shows the PAS spectrum of 'purified' sample of TNT vapor in a background of room air with a relative humidity of about 40% at 25 °C. The TNT detection limit is estimated to be ~0.1 ppb (S/N of 1) and corresponds to saturated TNT vapor pressure at 5 °C.

6.4. Quartz-enhanced photoacoustic spectroscopy

The intensity of an acoustic vibration induced by laser radiation in a gas-filled resonant cavity is determined by the following equation:

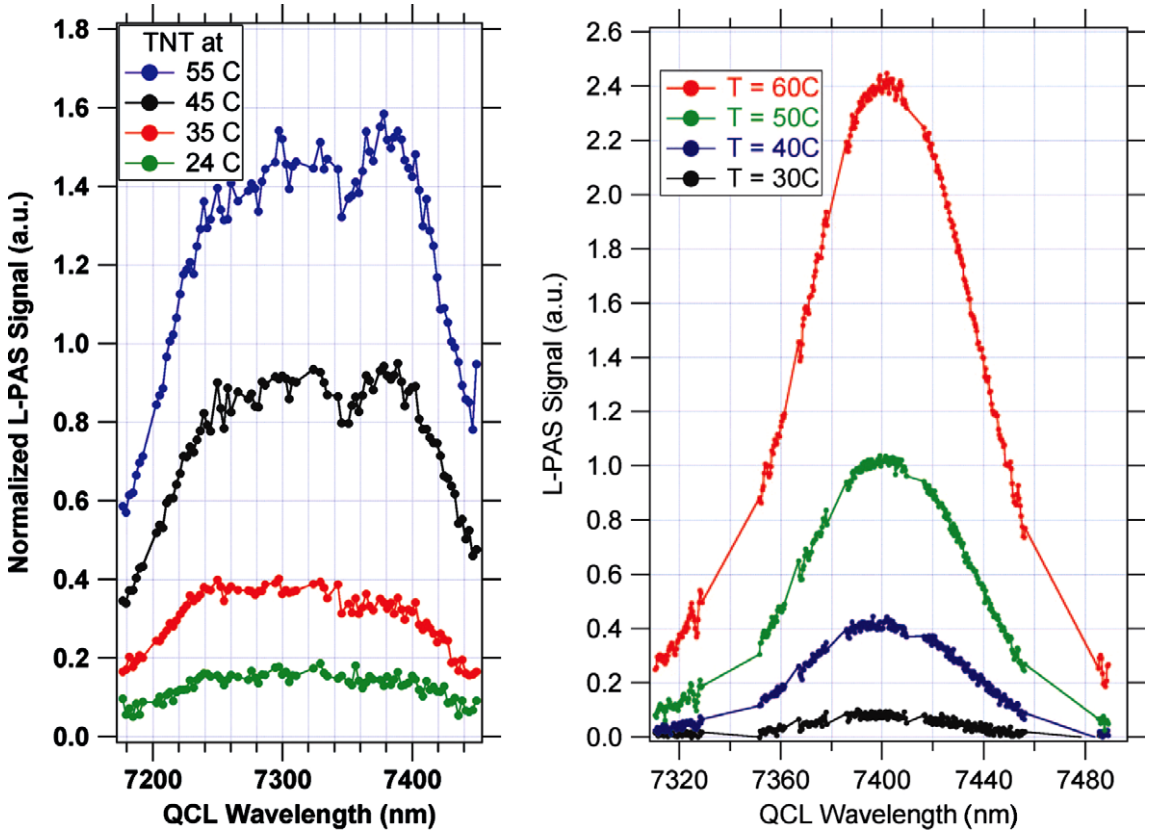

Fig. 11. TNT L-PAS spectra at different temperatures. Left: Fresh sample of commercial TNT8. Right: Spectra of the same sample after 48 h of dry air purge. (From Ref. [24] Copyright PNAS 2006).

$$p = k\frac{W}{V} \times \frac{Q}{\pi f} \tag{1}$$

Here p is the pressure amplitude of the acoustic vibration, k is a dimensionless coefficient dependent on the properties of the gas and a particular acoustic cavity design, W is the absorbed optical power, V is the acoustic mode volume, Q is the quality factor of the cavity and f is the resonant frequency of the cavity. A factor $Q/\pi f$ is equal to the acoustic cavity ring-down or build-up time; thus, $WQ/\pi f$ represents an amount of energy stored in the acoustic cavity, and p is proportional to the energy density in the gas. This leads to the important conclusion that the magnitude of the PAS signal can be increased by reducing the resonator volume. Typically, the basic design element of a photoacoustic cavity is a cylindrical channel along the laser beam. In this case,

$$W/V = \alpha I/(\pi r^2 l) = \alpha/(\pi r^2) \tag{2}$$

where l is the channel length, r is its radius and α is the optical absorption coefficient. It follows from (2) that, contrary to LAS, the useful signal (pressure amplitude) does not directly depend on the optical path in the sensor. This fact opens up an opportunity of creating truly miniature and still highly sensitive absorption detection modules, comparable in size with a semiconductor laser.

The conventional approach to the photoacoustic detector (spectrophone) design has limitations which do not allow reducing V below ~10 cm^3. The overall spectrophone dimensions, including sound isolation and buffer gas volumes, are typically ~10 cm or more, which is much larger than the QCL size.

A breakthrough in volume and size was achieved with a technique named quartz-enhanced photoacoustic spectroscopy, or QEPAS. QEPAS is based on using a quartz tuning fork (QTF, Fig. 12) as an acoustic transducer [83,112]. A QTF is cut out of a quartz monocrystal and properly oriented with respect to crystallographic axes. Quartz is a piezoelectric material, and therefore electrical charges are generated on its surfaces when the crystal is mechanically deformed. Metal films deposited on the surfaces collect these charges, which then can be measured either as a voltage or as a current, depending on the electronic circuit used. Hence, a QTF can be considered either as a mechanical or as an electrical oscillator.

The QTFs were originally designed for use in electronic clocks as frequency standards. The majority of commercially produced QTFs have a resonance at f = 32.8 kHz. So far, only QTFs at this frequency have been used in QEPAS sensors. Because of their long history of design refinements and mass production, QTFs provide both low cost and a number of unique properties, such as:

– High Q factor, typically ~100 000 in vacuum and ~10 000 at atmospheric pressure.

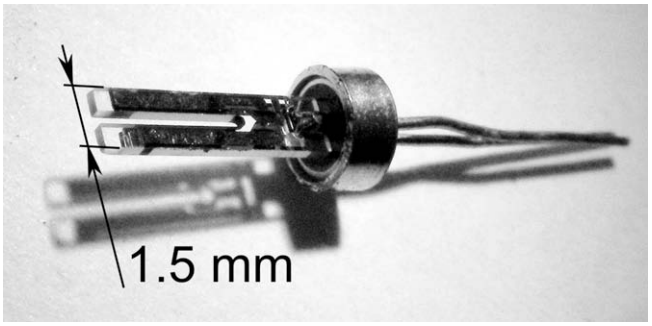

Fig. 12. Photograph of a quartz tuning fork. QTFs of this geometry was used in most QEPAS studies carried out in Rice University.

- Large dynamic range. The relation between electrical response and mechanical deformation has been shown to be linear up to the breakdown deformation of $\sim 10^{-2}$ cm tip displacement from the equilibrium position. At the same time, thermal noise of the QTF is readily observed and corresponds to $\sim 10^{-10}$ cm tip displacement.
- Wide temperature range. QTFs have been used in superfluid He at 1.56 K [113] and can potentially operate up to ~700 K where the piezoelectric effect vanishes.
- Spatial selectivity. The QTF is designed in such a way that the electrical signal is generated only when the two tines move in opposite directions. Therefore, it is mostly sensitive to a sound source positioned in a 0.3 mm gap between the tines.

This last property determines the preferred scheme for photoacoustic excitation of a QTF: the laser beam passes between the QTF prongs, as shown in Fig. 13a. In this case, the probed optical path is only as long as thickness of the QTF, or ~0.3 mm. Such a configuration can be useful when the excitation radiation cannot be shaped into a near-Gaussian beam, like for example for spatially multimode lasers. It was used in some experimental works and theoretically analyzed in [114].

The sensitivity can be significantly improved using a configuration shown in Fig. 13b, where two pieces of rigid tubing are added to confine the optically generated acoustic vibrations in the gas. Under certain conditions, these tubes can act as an additional (with respect to QTF) acoustic resonator. While the behavior of this system is quite complex and not yet fully theoretically understood, it was shown experimentally [115] that the configuration (b) yields 10–20 times improvement of the signal-to-noise ratio (SNR) compared to configuration (a). Sensor dimensions remain small, because the combined length of the microresonator tubes is between 5 and 10 mm with a tube inner diameter of 0.4–0.8 mm. Most QEPAS based sensors utilize configuration (Fig. 13b). Other QEPAS spectrophone configurations are also possible [116].

Like conventional photoacoustic spectroscopy, QEPAS does not require optical detectors such as photodiodes and can be used in different spectral regions with little or no modification to the spectrophone. This feature is especially attractive for gas sensing in the 5–20 μm region, where the availability of high-performance optical detectors is limited, and cryogenic cooling is often required. The QEPAS technique also benefits from the high optical power of QCLs.

Most QEPAS sensors to date have been based on 2*f* wavelength modulation (WM) spectroscopy, which provides complete suppression of any coherent acoustic background that might be created when stray modulated radiation is absorbed by nonselective absorbers, such as the gas cell elements and the QTF itself. For QEPAS 2*f* WM spectroscopy, the laser wavelength must be modulated at half the resonant frequency of the QTF. In this case, the noise floor is determined by thermal noise of the QTF [117].

Due to its high *Q* factor, the QTF used as a detector has a long response time, determined by the equation $\tau = Q/\pi f$. Therefore, the technique of rapid spectral scans often used in LAS is not applicable. However, 2*f* WM QEPAS produces background-free data, eliminating the need of spectral scanning to determine the baseline level. Hence, while slow spectral scans can be performed and are actually useful for laboratory studies, field-application oriented sensors are designed to have the laser locked to the absorption line of the target gas and to continuously monitor the signal resulting from the optical absorption at that wavelength.

The first QEPAS based trace gas sensing experiments using QCLs and ICLs were performed in 2004 [118–120]. In [119], a liquid nitrogen cooled CW DFB QCL at 4.55 μm was used to detect N_2O (2195.633 cm^{-1} absorption line) and CO (2196.664 cm^{-1}). This work revealed that molecular energy transfer processes leading to thermalization of excess molecular vibrational energy (V-T relaxation) have a significant impact on the sensor performance. The observed QEPAS signals in N_2O:N_2 and CO:N_2 mixtures were much lower than expected based on the relevant absorption coefficients. This phenomenon is well known in conventional photoacoustic spectroscopy, see for example [121]. If the V-T relaxation rate is lower than the optical excitation modulation frequency, the amplitude of the optically induced acoustic signal is reduced. This effect is more significant for QEPAS due to the high modulation frequency of 32.8 kHz. It is more likely to occur with small (2–3 atoms) molecules, which do not have a dense ladder of energy levels to facilitate V-T relaxation. Sometimes, a small addition of other species eliminates the V-T relaxation bottleneck. In [119], adding 5% SF_6 to a N_2O:N_2 mixture increased the signal 10 times and resulted in a 4 ppbv detection sensitivity in 0.0625 Hz bandwidth with 11 mW of laser power. In many practical applications, the presence of small amounts of H_2O vapor in the analyzed gas solves the slow relaxation problem.

While V-T relaxation can complicate QEPAS based sensing in some cases, the same phenomenon can be used in other situations to add to the chemical selectivity. It was noticed already in 1946 [122] and experimentally confirmed in 1948 [123] that the phase of the photoacoustic signal can be used to measure the V-T relaxation rate. Thus, this rate or the related phase shift can be used as an additional spectroscopic parameter to distinguish species with overlapping absorption spectra. Such an approach was used in [120] to measure trace CO impurity concentrations in 100% propylene.

QEPAS excitation can also be performed in an amplitude modulation (AM) mode, although in this case a coherent acoustic background should be expected. This background is directly

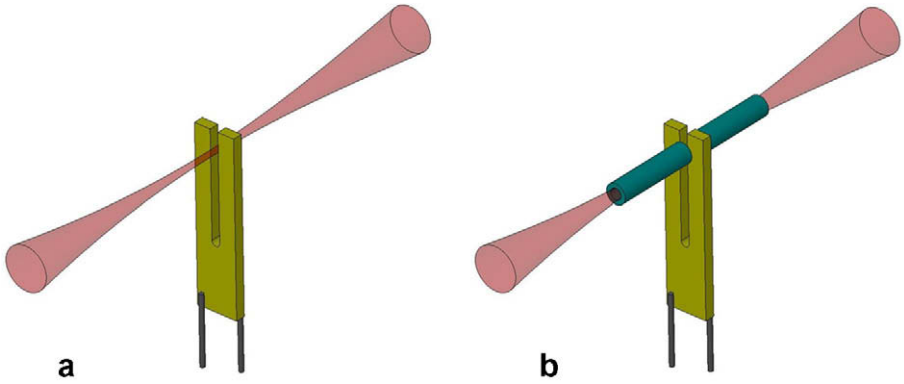

Fig. 13. The QTF based spectrophones: (a) simplest configuration and (b) improved configuration with an acoustic resonator formed by two pieces of rigid tubing.

proportional to the laser power reaching the spectrophone. Therefore, the sensitivity limit is no longer determined by the QTF thermal noise alone but also by laser power fluctuations and spurious interference features. The AM mode must be used if the absorption feature of interest is spectrally so wide that fast modulation of the laser wavelength across this feature is not possible. This is often the case for large or heavy molecules, when individual ro-vibrational transitions are not resolved and absorption bands look unstructured. In AM mode, there are several choices of the modulation method. The first QEPAS gas sensing experiments using amplitude modulation on a congested band of tetrafluoroethane using pulsed lasers were reported in 2006 [124]. More recently an EC-QCL tunable in the 1120–1240 cm^{-1} range was utilized to quantify trace concentrations of Freon 125 (pentafluoroethane) and acetone in nitrogen, added individually or simultaneously [125]. The figure of merit in photoacoustic spectroscopy is the noise equivalent absorption coefficient at unit bandwidth at unit laser power and is designated NNEA. An NNEA = 2.64×10^{-9} cm^{-1} $W/Hz^{1/2}$ comparable to the best results of conventional PAS and corresponding to ppbv levels of the Freon 125 was obtained using separate measurements of coherent acoustic background in pure nitrogen and its subsequent subtraction from the signal.

6.5. Faraday rotation spectroscopy with quantum cascade lasers

In the vicinity of an optical transition, there is an anomaly in the index of refraction. Faraday rotation spectroscopy (FRS) [126,127] takes advantage of dispersion effects of paramagnetic species (such as NO, NO_2, OH^- or O_2). When an external magnetic field is applied in the same direction as the light propagation, paramagnetic molecules exhibit magnetic circular birefringence (MCB). This implies that the refractive index is different for left-handed and right-handed circularly polarized waves traveling in the medium. Thus with the transition split by the magnetic field, linearly polarized light, which is a superposition of two circularly polarized waves, is affected by different Zeeman components of the transitions, and MCB can be observed as rotation of the polarization plane of a linearly polarized laser radiation. Such a polarization rotation, which is observed strongly only around absorption lines, is proportional to the column density of paramagnetic species. The polarization rotation angle can be detected very precisely using a modulated magnetic field and phase sensitive detection techniques.

The basic FRS setup is shown in Fig. 14. The FRS signal is measured by placing the sample between two Rochon polarizers, so that the Faraday rotation can be detected as intensity modulation of the light emerging from the second polarizer (analyzer). Two methods have been used for polarization rotation measurement: the so called 90-degree method uses two polarizers with almost crossed polarization axes and a single photodetector for sensing of the transmitted light intensity [126], and the second measurement method [127] orients the analyzer at 45° splitting the beam into two polarizations and uses two balanced detectors to detect that the beams go out of balance when MCB is present. Signal-to-noise (SNR) enhancement is achieved in slightly different ways for the two methods, but fundamentally both are based upon efficient suppression of laser amplitude noise while maximizing the Faraday rotation signal. In both methods, the spectral shape of the FRS signal is the sum of the differences between Zeeman shifted dispersion curves. Since the polarization rotation and thus the variation of the analyzer transmission exist only when the nitric oxide molecules are present, FRS is considered a zero optical background technique and provides ultra-high sensitivities.

In the 90-degree method, suppression of the laser noise is achieved by nearly crossing the analyzer, thus reducing the amount of laser amplitude noise arriving at the detector. The signal is also suppressed by crossing the polarizers, but SNR enhancement is obtained, because the signal is an approximately linear function of the displacement of the analyzer angle from minimum transmitted light, while the noise has a quadratic dependence upon angle. Significant improvements in SNRs have been demonstrated even for relatively noisy laser sources such as color center lasers [126]. The application of quantum cascade lasers, which are much more compact, powerful and exhibit much lower amplitude noise than, e.g. color center laser sources, is [128] an important step in adopting the FRS technology for applications outside the research laboratory.

Depending on the ratio of laser intensity fluctuations to detector noise at the modulation frequency, the signal-to-noise ratio can be limited either by detector noise for quiet sources or by polarizer quality for noisier sources. There is an optimum analyzer angle for the 90-degree method, which depends upon detector noise or polarizer quality. This has been analyzed in detail (see [128, Supplementary material]).

The FRS signal can be modeled [129,130] based on parameters of the molecular transition, including magnetic moment and experimental conditions (sample pressure, temperature, magnetic field amplitude, optical path-length, etc.). Precise modeling of the FRS signals has a great potential for providing consumable-free calibration, which is particularly attractive for field sensing applications.

An experiment using a cryogenically cooled indium-antimonide (InSb) detector with only 44 cm optical path-length yielded a 1σ minimum NO detection limit of 380 pptv with 1 s lock-in time constant [128]. This corresponds to 5.9×10^{-8} equivalent minimum detectable fractional absorption calculated for this NO $Q_{3/2}(3/2)$ line. The best current state-of-the-art LAS systems require more than ten times the path-length in order to provide a comparable sensitivity.

FRS can be applied to most molecular species possessing a permanent magnetic dipole moment. Examples are nitric oxide, oxygen, nitrogen dioxide and many radicals, e.g. hydroxyl radical. Semiconductor laser sources and in particular QCLs, which operate in the

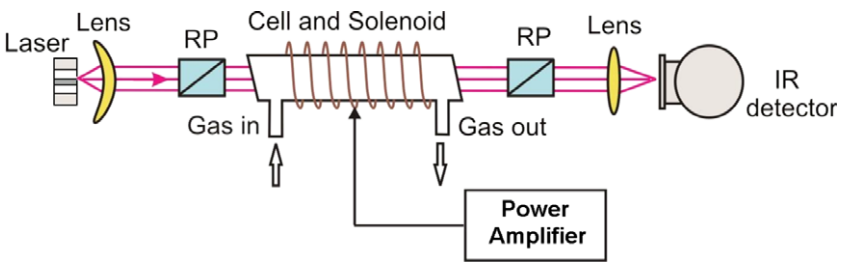

Fig. 14. Schematic of the 90° FRS scheme. The two Rochon polarizers (RP) are nearly crossed at angle determined to give the best S/N.

mid-IR molecular fingerprint region, in combination with ultra-sensitive FRS, can provide particularly attractive technology for compact and accurate trace-gas detectors for true field applications.

7. Future prospects

While the tuning range of QCLs was only a few cm^{-1}, spectroscopic opportunities were essentially limited to monitoring specific species. Thus, besides trace gas monitoring of small molecules, the only opportunities appeared to be monitoring species in chemical gas kinetics or doing saturation spectroscopy on a few particular molecular lines [131–136]. Once it became possible to construct EC sources covering two or even three hundred cm^{-1}, the monitoring with some selectivity of larger molecules with congested rotational spectra having no mid-IR rotational lines resolved (the vast majority of molecules) became possible. In most cases, IR molecular spectra in condensed phases (liquids or solids) are generally rather broad and featureless as well. QCL spectroscopy has been applied to a small number of such cases condensed phase cases, such as functional group characterization of liquid chromatography peaks [137], detecting trace water in solvents [138] and photoacoustic spectroscopy of solids [139].

It seems unlikely that QCLs will be used to any great extent in Doppler-limited investigations of the high resolution spectra of stable molecules because high resolution FTIR is equally powerful and still much easier (though with a high entry price, especially for high-resolution models such as Bruker IFS 125 Series with resolution $\sim$0.001 cm^{-1}). Although FTIR is quite sensitive, laser spectroscopy is much more sensitive because the intrinsic brightness per unit frequency interval of the laser is so much greater than any practical blackbody source. Thus, QCL spectroscopy has a bright future in the study of transient species such as radicals or ions. Such species typically can be prepared in steady state only in very low concentrations or only transiently (by flash photolysis, for example) in higher concentrations.

Laser sources generally are much more suitable than FTIR for absorption spectroscopy in supersonic jets for several reasons (especially for studies of transient species, including weakly bound species). As noted above, sensitivity for a given path-length is better, the coherent beam is easier to multi-pass through the small cross-section of the jet, and the QCL's small linewidth matches the smaller linewidths that can be found in a slit jet.

QCLs because of their relatively high power and narrow linewidths are extremely well suited to moving populations between states and to depositing energy selectively. With the ability to obtain tunable radiation throughout most of the mid-IR, there is a bright future for the application of QCLs to multiple resonance experiments, to molecular dynamics experiments, to molecular beam resonance studies, to helium droplet spectroscopy, to hole burning in heterogeneously broadened solid state systems, and for driving infrared photochemistry of materials isolated in cryogenic matrices.

Progress in the development of QCLs in the 15 years since their first realization has been breathtakingly rapid. Now that the technology has grown so much, we can expect equally breathtaking progress in their application in many areas of chemical physics.

Acknowledgments

The Rice University and Princeton groups acknowledge the financial support from a NSF ERC MIRTHE award. F. Tittel and G. Wysocki received a sub-contract from a DOE STTR grant from Aerodyne Research Inc., The Rice group also acknowledges support from a grant C-0586 from The Welch Foundation, and a grant from the National Aeronautics and Space Administration. F. Capasso acknowledges collaborations with B. Lee, M.A. Belkin, L. Diehl, C. Pfluegl, Q.J. Wang, J. Kansky, A.K. Goyal, and A. Sanchez and support from DARPA and the Airforce Office for Scientific Research.

References

[1] J. Faist, F. Capasso, D.L. Sivco, A.L. Hutchinson, A.Y. Cho, Science 264 (1994) 553.
[2] R.F. Kazarinov, R.A. Suris, Sov. Phys. Semicond. 5 (1971) 707.
[3] C. Gmachl, F. Capasso, D.L. Sivco, A.Y. Cho, Rep. Prog. Phys. 64 (2001) 1533.
[4] F. Capasso et al., IEEE J. Sel. Top. Quantum Electron. 6 (2000) 931.
[5] M. Beck et al., Science 295 (2002) 301.
[6] M. Razeghi, IEEE J. Sel. Top. Quantum Electron. 15 (2009) 941.
[7] M. Razeghi, Proc. SPIE 7230 (2009) 723011.
[8] A. Lyakh et al., Appl. Phys. Lett. 95 (2009) 141113.
[9] R. Maulini et al., Appl. Phys. Lett. 95 (2009) 151112.
[10] J. Faist et al., Appl. Phys. Lett. 70 (1997) 2670.
[11] J. Faist, F. Capasso, C. Sirtori, D.L. Sivco, A.L. Hutchinson, A.Y. Cho, Electron. Lett. 32 (1996) 560.
[12] J. Faist et al., J. Cryst. Growth 175 (1997) 22.
[13] C. Sirtori, J. Faist, F. Capasso, D.L. Sivco, A.L. Hutchinson, A.Y. Cho, IEEE Photon. Technol. Lett. 9 (1997) 294.
[14] S.G. Patterson, G.S. Petrich, R.J. Ram, L.A. Kolodziejski, Electron. Lett. 35 (1999) 395.
[15] S. Slivken, A. Matlis, C. Jelen, A. Rybaltowski, J. Diaz, M. Razeghi, Appl. Phys. Lett. 74 (1999) 173.
[16] C. Gmachl et al., Electron. Lett. 36 (2000) 723.
[17] F.Q. Liu et al., Electron. Lett. 36 (2000) 1704.
[18] M. Rochat, D. Hofstetter, M. Beck, J. Faist, Appl. Phys. Lett. 79 (2001) 4271.
[19] J. Faist, D. Hofstetter, M. Beck, T. Aellen, M. Rochat, S. Blaser, IEEE J. Quantum Electron. 38 (2002) 533.
[20] S. Anders, W. Schrenk, C. Pflugl, E. Gornik, G. Strasser, C. Becker, C. Sirtori, IEE Proc. Optoelectron. 150 (2003) 282.
[21] D.A. Carder et al., Appl. Phys. Lett. 82 (2003) 3409.
[22] G. Wysocki, R.F. Curl, F.K. Tittel, R. Maulini, J.M. Bulliard, J. Faist, Appl. Phys. B 81 (2005) 769.
[23] R. Maulini, A. Mohan, M. Giovannini, J. Faist, E. Gini, Appl. Phys. Lett. 88 (2006) 201113.
[24] M.B. Pushkarsky, I.G. Dunayevskiy, M. Prasanna, A.G. Tsekoun, R. Go, C.K.N. Patel, Proc. Natl Acad. Sci. USA 103 (2006) 19630.
[25] M. Pushkarsky, A. Tsekoun, I.G. Dunayevskiy, R. Go, C.K.N. Patel, Proc. Natl Acad. Sci. USA 103 (2006) 10846.
[26] G. Wysocki et al., Appl. Phys. B 92 (2008) 305.
[27] A. Wittmann, A. Hugi, E. Gini, N. Hoyler, J. Faist, IEEE J. Quantum Electron. 44 (2008) 1083.
[28] B.G. Lee et al., IEEE J. Quantum Electron. 45 (2009) 554.
[29] B.G. Lee et al., IEEE Photon. Technol. Lett. 21 (2009) 914.
[30] M. Troccoli et al., J. Lightw. Technol. 26 (2008) 3534.
[31] A. Lyakh et al., Appl. Phys. Lett. 92 (2008) 111110.
[32] M.A. Belkin et al., IEEE J. Sel. Top. Quantum Electron. 15 (2009) 952.
[33] B.S. Williams, Nat. Photon. 1 (2007) 517.
[34] S. Mukherjee, Z.S. Shi, IETE Tech. Rev. 26 (2009) 236.
[35] R.H. Rediker, I. Melngailis, A. Mooradian, IEEE J. Quantum Electron. 20 (1984) 602.
[36] D. Hofstetter, M. Beck, T. Aellen, J. Faist, Appl. Phys. Lett. 78 (2001) 396.
[37] C. Gmachl, D.L. Sivco, J.N. Baillargeon, A.L. Hutchinson, F. Capasso, A.Y. Cho, Appl. Phys. Lett. 79 (2001) 572.
[38] C. Gmachl, D.L. Sivco, R. Colombelli, F. Capasso, A.Y. Cho, Nature 415 (2002) 883.
[39] A. Hugi et al., Appl. Phys. Lett. 95 (2009) 061103.
[40] M. Pushkarsky, M. Weida, T. Day, D. Arnone, R. Pritchett, D. Caffey, S. Crivello, Proc. SPIE 6871 (2008) 68711X/1.
[41] B.G. Lee et al., Opt. Express 17 (2009) 16216.
[42] F. Capasso, N. Yu, E. Cubukcu, E. Smythe, Opt. Photon. News 20 (2009) 22.
[43] J. Faist, F. Capasso, D.L. Sivco, A.L. Hutchinson, S.N.G. Chu, A.Y. Cho, Appl. Phys. Lett. 72 (1998) 680.
[44] M.P. Semtsiv, M. Ziegler, S. Dressler, W.T. Masselink, N. Georgiev, T. Dekorsy, M. Helm, Appl. Phys. Lett. 85 (2004) 1478.
[45] J. Devenson, O. Cathabard, R. Teissier, A.N. Baranov, Appl. Phys. Lett. 91 (2007) 251102.
[46] X. Marcadet, C. Renard, M. Carras, M. Garcia, J. Massies, Appl. Phys. Lett. 91 (2007) 161104.
[47] M.P. Semtsiv, S. Dressler, W.T. Masselink, IEEE J. Quantum Electron. 43 (2007) 42.
[48] M.P. Semtsiv, M. Wienold, S. Dressler, W.T. Masselink, Appl. Phys. Lett. 90 (2007) 051111.
[49] J. Devenson, O. Cathabard, R. Teissier, A.N. Baranov, Appl. Phys. Lett. 91 (2007) 141106.
[50] J.P. Commin, D.G. Revin, S.Y. Zhang, A.B. Krysa, J.W. Cockburn, Appl. Phys. Lett. 95 (2009) 111113.
[51] O. Cathabard, R. Teissier, J. Devenson, A.N. Baranov, Electron. Lett. 45 (2009) 1028.
[52] J.S. Yu, A. Evans, S. Slivken, S.R. Darvish, M. Razeghi, IEEE Photon. Technol. Lett. 17 (2005) 1154.

[53] J.S. Yu, A. Evans, S. Slivken, S.R. Darvish, M. Razeghi, Appl. Phys. Lett. 88 (2006) 251118.
[54] S.Y. Zhang, D.G. Revin, J.W. Cockburn, K. Kennedy, A.B. Krysa, M. Hopkinson, Appl. Phys. Lett. 94 (2009) 031106.
[55] R.Q. Yang, Superlattices Microstruct. 17 (1995) 77.
[56] M. Kim et al., Appl. Phys. Lett. 92 (2008) 191110.
[57] R. Colombelli et al., Appl. Phys. Lett. 78 (2001) 2620.
[58] G. Scalari, C. Walther, M. Fischer, R. Terazzi, H. Beere, D. Ritchie, J. Faist, Laser Photon. Rev. 3 (2009) 45.
[59] S. Kumar, Q. Hu, J.L. Reno, Appl. Phys. Lett. 94 (2009) 131105.
[60] A. Wade, G. Fedorov, D. Smirnov, S. Kumar, B.S. Williams, Q. Hu, J.L. Reno, Nat. Photon. 3 (2009) 41.
[61] M.A. Belkin, F. Capasso, F. Xie, A. Belyanin, M. Fischer, A. Wittmann, J. Faist, Appl. Phys. Lett. 92 (2008) 201101.
[62] A. Soibel, C. Gmachl, D.L. Sivco, M.L. Peabody, A.M. Sergent, A.Y. Cho, F. Capasso, Appl. Phys. Lett. 83 (2003) 24.
[63] B.G. Lee, M.A. Belkin, R. Audet, J. MacArthur, L. Diehl, C. Pflugl, F. Capasso, Appl. Phys. Lett. 91 (2007) 231101.
[64] A. Wittmann, T. Gresch, E. Gini, L. Hvozdara, N. Hoyler, M. Giovannim, J. Faist, IEEE J. Quantum Electron. 44 (2008) 36.
[65] R. Maulini et al., Electron. Lett. 45 (2009) 107.
[66] R. Maulini, D.A. Yarekha, J.M. Bulliard, M. Giovannini, J. Faist, Opt. Lett. 30 (2005) 2584.
[67] T. Gensty, W. Elsäßer, C. Mann, Opt. Express 13 (2005) 2032.
[68] T. Gensty, W. Elsäßer, Opt. Commun. 256 (2005) 171.
[69] F. Rana, P. Mayer, R.J. Ram, J. Opt. B: Quantum Semiclass. Opt. 6 (2004) S771.
[70] F. Rana, R.J. Ram, Phys. Rev. B 65 (2002) 125313.
[71] N. Mustafa, L. Pesquera, K.A. Shore, J. Mod. Opt. 47 (2000) 1825.
[72] D. Weidmann, G. Wysocki, Opt. Express 17 (2009) 248.
[73] Y. Takagi, N. Kumazaki, M. Ishihara, K. Kasahara, A. Sugiyama, N. Akikusa, T. Edamura, Electron. Lett. 44 (2008) 860.
[74] D. Weidmann, K. Smith, B. Ellison, Appl. Opt. 46 (2007) 947.
[75] T. Gensty, J. von Staden, W. Elsäßer, Tech. Mess. 72 (2005) 380.
[76] S. Bartalini et al., arxiv:/arXiv:0912.2683v1 ([physics.optics] 14.12.2009).
[77] D.S. Elliott, R. Roy, S.J. Smith, Phys. Rev. A 26 (1982) 12.
[78] M. Yamanishi, T. Edamura, K. Fujita, N. Akikusa, H. Kan, IEEE J. Quantum Electron. 44 (2008) 12.
[79] T. Aellen et al., Appl. Phys. Lett. 89 (2006) 091121.
[80] J. Faist, F. Capasso, C. Sirtori, D.L. Sivco, A.L. Hutchinson, A.Y. Cho, Appl. Phys. Lett. 67 (1995) 3057.
[81] N. Kumazaki, Y. Takagi, M. Ishihara, K. Kasahara, A. Sugiyama, N. Akikusa, T. Edamura, Appl. Phys. Lett. 92 (2008) 121104.
[82] J. von Staden, T. Gensty, W. Elsäßer, G. Giuliani, C. Mann, Opt. Lett. 31 (2006) 2574.
[83] A.A. Kosterev, Y.A. Bakhirkin, R.F. Curl, F.K. Tittel, Opt. Lett. 27 (2002) 1902.
[84] J.U. White, J. Opt. Soc. Am. 32 (1942) 285.
[85] D.R. Herriott, H.J. Schulte, Appl. Opt. 4 (1965) 883.
[86] J.B. McManus, P.L. Kebabian, W.S. Zahniser, Appl. Opt. 34 (1995) 3336.
[87] S.C. Herndon et al., J. Geophys. Res.-Atmos. 112 (2007) S1003.
[88] R. Jimenez, S. Herndon, J.H. Shorter, D.D. Nelson, J.B. McManus, M.S. Zahniser, Proc. SPIE 5738 (2005) 318.
[89] M.S. Zahniser et al., Proc. SPIE 7222 (2009) 72220H.
[90] L.S. Rothman et al., J. Quant. Spectrosc. Radiat. Transfer 82 (2003) 5.
[91] S.C. Wofsy, B. Daube, R. Jimenez, S. Park, E.A. Kort, AGU Fall Meeting 2008 89 (2008) A43F.
[92] B. Tuzson et al., Appl. Phys. B 92 (2008) 451.
[93] D.D. Nelson, J.B. McManus, S.C. Herndon, M.S. Zahniser, B. Tuzson, L. Emmenegger, Appl. Phys. B 90 (2008) 301.
[94] A. O'Keefe, D.A.G. Deacon, Rev. Sci. Instrum. 59 (1988) 2544.
[95] A.J. Ramponi, F.P. Milanovich, T. Kan, D. Deacon, Appl. Opt. 27 (1988) 4606.
[96] J.J. Scherer, J.B. Paul, A. O'Keefe, R.J. Saykally, Chem. Rev. 97 (1997) 25.
[97] M. Mazurenka, A.J. Orr-Ewing, R. Peverall, G.A.D. Ritchie, Ann. Rep. Prog. Chem. Sec. C 101 (2005) 100.
[98] J. Manne, O. Sukhorukov, W. Jager, J. Tulip, Appl. Opt. 45 (2006) 9230.
[99] B.A. Paldus et al., Opt. Lett. 25 (2000) 666.
[100] A.A. Kosterev et al., Appl. Opt. 40 (2001) 5522.
[101] Y.A. Bakhirkin et al., Appl. Phys. B 82 (2006) 149.
[102] G.S. Engel, W.S. Drisdell, F.N. Keutsch, E.J. Moyer, J.G. Anderson, Appl. Opt. 45 (2006) 9221.
[103] A. O'Keefe, Chem. Phys. Lett. 293 (1998) 331.
[104] A. O'Keefe, J.J. Scherer, J.B. Paul, Chem. Phys. Lett. 307 (1999) 343.
[105] J.B. Paul, L. Lapson, J.G. Anderson, Appl. Opt. 40 (2001) 4904.
[106] M.R. McCurdy, Y. Bakhirkin, G. Wysocki, F.K. Tittel, J. Biomed. Opt. 12 (2007) 34034.
[107] D.S. Sayres et al., Rev. Sci. Instrum. 80 (2009) 044102.
[108] M.B. Pushkarsky, M.E. Webber, C.K.N. Patel, Appl. Phys. B 77 (2003) 381.
[109] M.B. Pushkarsky, M.E. Webber, T. Macdonald, C.K.N. Patel, Appl. Phys. Lett. 88 (2006) 044103.
[110] National Air Quality and Emission Trends Report, 2003, Special Studies Edition, US Government Printing Office, Washington, DC, 2003.
[111] M.W. Todd et al., Appl. Phys. B 75 (2002) 367.
[112] A.A. Kosterev, F.K. Tittel, D.V. Serebryakov, A.L. Malinovsky, I.V. Morozov, Rev. Sci. Instrum. 76 (2005) 043105.
[113] J. Rychen et al., Rev. Sci. Instrum. 71 (2000) 1695.
[114] N. Petra, J. Zweck, A.A. Kosterev, S.E. Minkoff, D. Thomazy, Appl. Phys. B 94 (2009) 673.
[115] L. Dong, A.A. Kosterev, D. Thomazy, F.K. Tittel, in: The Conference on Lasers and Electro-Optics (CLEO)/The International Quantum Electronics Conference (IQEC), Baltimore, MD, USA, 2009.
[116] K. Liu, X.Y. Guo, H.M. Yi, W.D. Chen, W.J. Zhang, X.M. Gao, Opt. Lett. 34 (2009) 1594.
[117] R.D. Grober et al., Rev. Sci. Instrum. 71 (2000) 2776.
[118] M. Horstjann et al., Appl. Phys. B 79 (2004) 799.
[119] A.A. Kosterev, Y.A. Bakhirkin, F.K. Tittel, Appl. Phys. B 80 (2005) 133.
[120] A.A. Kosterev, Y.A. Bakhirkin, F.K. Tittel, S. Blaser, Y. Bonetti, L. Hvozdara, Appl. Phys. B 78 (2004) 673.
[121] R.A. Rooth, A.J.L. Verhage, L.W. Wouters, Appl. Opt. 29 (1990) 3643.
[122] G. Gorelik, Dokl. Akad. Nauk SSSR 54 (1946) 779.
[123] P.V. Slobodskaya, Izvest. Akad. Nauk SSSR 12 (1948) 656.
[124] M.D. Wojcik, M.C. Phillips, B.D. Cannon, M.S. Taubman, Appl. Phys. B 85 (2006) 307.
[125] R. Lewicki, G. Wysocki, A.A. Kosterev, F.K. Tittel, Opt. Express 15 (2007) 7357.
[126] G. Litfin, C.R. Pollock, R.F. Curl, F.K. Tittel, J. Chem. Phys. 72 (1980) 6602.
[127] H. Adams, D. Reinert, P. Kalkert, W. Urban, Appl. Phys. B 34 (1984) 179.
[128] R. Lewicki, J.H. Doty, R.F. Curl, F.K. Tittel, G. Wysocki, Proc. Natl Acad. Sci. USA 106 (2009) 12587.
[129] H. Ganser, W. Urban, A.M. Brown, Mol. Phys. 101 (2003) 545.
[130] W. Herrmann, W. Rohrbeck, W. Urban, Appl. Phys. A 22 (1980) 71.
[131] S. Bartalini, S. Borri, P. De Natale, Opt. Express 17 (2009) 7440.
[132] N. Mukherjee, C.K.N. Patel, Chem. Phys. Lett. 462 (2008) 10.
[133] N. Mukherjee, R. Go, C.K.N. Patel, Appl. Phys. Lett. 92 (2008) 111116.
[134] F. Bielsa et al., J. Mol. Spectrosc. 247 (2008) 41.
[135] A. Castrillo, E. De Tommasi, L. Gianfrani, L. Sirigu, J. Faist, Opt. Lett. 31 (2006) 3040.
[136] J.T. Remillard et al., Opt. Express 7 (2000) 243.
[137] A. Edelmann, C. Ruzicka, J. Frank, B. Lendl, W. Schrenk, E. Gornik, G. Strasser, J. Chromatogr. A 934 (2001) 123.
[138] A. Ouvrard, K. O'Dwyer, B.D. MacCraith, Appl. Spectrosc. 62 (2008) 1349.
[139] Q. Wen, K.H. Michaelian, Opt. Lett. 33 (2008) 1875.

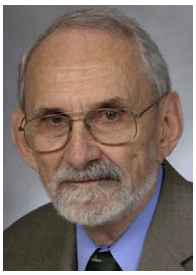

Robert F. Curl is Kenneth S. Pitzer-Schlumberger Professor of Natural Sciences Emeritus and University Professor Emeritus at Rice University. He attended Rice Institute receiving the B.A. from Rice in 1954 and the Ph.D. from Berkeley in 1957. After a postdoctoral at Harvard, he joined the faculty at Rice where he has been ever since. He is a member of the National Academy of Sciences, European Academy of Arts and Sciences, Phi Beta Kappa, Phi Lambda Upsilon, and Sigma Xi. He is a Fellow of the American Academy of Arts and Sciences, a Fellow of the Optical Society of America, Fellow of the Royal Society of Chemistry, and Honorary Fellow of the Royal Society of New Zealand. Jointly with Richard Smalley and Harold Kroto, he received the Nobel Prize in Chemistry in 1996. He has received a number of other awards. His primary research interests have been in molecular spectroscopy, chemical kinetics, and the chemistry of elemental carbon.

Federico Capasso is the Robert L. Wallace Professor of Applied Physics at Harvard University, which he joined in 2003 after a 26 years career at Bell Labs where he rose from postdoc to Vice President for Physical Research. He holds a Doctor of Physics degree from the University of Rome, Italy, 1973. His research includes the design of new artificial materials and novel devices, plasmonics, nanophotonics, and quantum electrodynamics. He pioneered band-structure engineering as a technique to design new heterostructure materials and devices. He is co-inventor of the quantum cascade laser, a fundamentally new light source, which has now been commercialized. Recent achievements include the first measurement of repulsive Casimir force and wavefront engineering of lasers using plasmonics. He has co-authored over 350 papers, edited four volumes, and holds over 60 US patents. He is a member of the National Academy of Sciences, the National Academy of Engineering, a Fellow of the American Academy of Arts and Sciences, an honorary member of the Franklin Institute, a Fellow of OSA, IEEE, SPIE, APS and AAAS. His awards include the King Faisal International Prize for Science, the American Physical Society Arthur Schawlow Prize, the Wetherill Medal of the Franklin Institute, the IEEE Edison Medal, the IEEE D. Sarnoff Award, the IEEE/LEOS Streifer Award, the Optical Society of America Robert Wood prize, the Rank Prize in Optoelectronics, the Material Research Society Medal, the Welker Medal, the Duddell Medal and Prize of the Institute of Physics (UK), the Newcomb Cleveland Prize of the American Association for the Advancement of Science, the 'Vinci of Excellence' LMVH Prize and the New York Academy of Sciences Award.

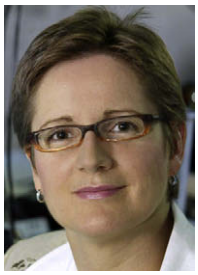

Claire Gmachl received the Ph.D. degree (sub auspicies praesidentis) in electrical engineering from the Technical University of Vienna, Austria, in 1995. In 1996, she joined Bell Laboratories, Lucent Technologies, Murray Hill, NJ, as Post-Doctoral Member of Technical Staff to work on Quantum Cascade laser devices and microcavity lasers. In March 1998 she became a Member of Technical Staff in the Semiconductor Physics Research Department and a Distinguished Member of Staff in 2002. In September 2003, she joined Princeton University as an Associate Professor in the Department of Electrical Engineering and adjunct faculty to PRISM; since July 2007 she is Full Professor at Princeton University. She is the Director of MIRTHE, the NSF Engineering Research Center on Mid-InfraRed Technologies for Health and the Environment. She has authored and co-authored more than 180 publications, has given more than 90 invited presentations at conferences and seminars, and holds 26 patents. She was presented with a Graduate Student Mentoring Award, Princeton University 2009, and is a Corresponding Member Abroad of the Austrian Academy of Sciences since 2008; she is an Associate Editor for Optics Express and a member of the IEEE/LEOS Board of Governors. She is a 2005 MacArthur Fellow. She has won various awards and is a member of several professional societies.

Anatoliy A. Kosterev is a Senior Faculty Fellow at the Electrical and Computer Engineering Department, Rice University. He received a M.Sc. degree in physics from the Moscow Institute of Physics and Technology in 1985 and a Ph.D. degree in physics from the Institute of Spectroscopy, Russian Academy of Sciences, in 1995 based on his investigations in the field of vibrational molecular dynamics. His current research mostly concerns chemical gas analysis by means of laser spectroscopy, and in particular, development of quartz enhanced photoacoustic spectroscopy that he invented in 2002. He is a member of the Optical Society of America.

Barry McManus is a principal scientist at Aerodyne Research Inc. and specializes in the development of infrared laser spectroscopic instrumentation. He received a Ph.D. in physics from MIT, studying nonlinear optical processes in semiconductors. Since joining Aerodyne Research, he has developed numerous laser instruments for trace gas sensing and has developed new methods for their use in field measurements. He is actively involved in designs for multi-pass optical cells and instruments which utilize them. He is the author of more than 50 refereed publications, and is a Fellow of the Optical Society of America.

Rafał Lewicki received his M.S. degree in Electronics from Wroclaw University of Technology, Wroclaw, Poland in 2005 and he is currently working toward a Ph.D. degree from the same university. In December 2005, he joined Laser Science Group at Rice University, Houston, TX as a visiting scholar. His research interest is trace gas detection using laser based spectroscopic techniques. His current activities focus on the implementation of quantum cascade laser based sensor platforms, enabling high resolution, selective and quantitative spectroscopic measurements for environmental and medical applications.

Michael Pushkarsky currently serves as a Senior Scientist at Daylight Solutions, a manufacturer of molecular detection and imaging products located in Poway, CA. He is responsible for the development and commercialization of sensors and lasers based on Daylight's quantum cascade laser technology. Prior to joining Daylight, he worked for start-up company, Pranalytica, where he was responsible for the development of advanced laser-based trace gas sensors. He received his Ph.D. in Chemical Physics from the Ohio State University, where his academic research was focused on laser spectroscopy of free radicals. He has authored over twenty peer-reviewed publications and holds several patents. His teams have been recognized with several academic and industry awards, most recently with the 2008 SPIE Prism Award for Photonics Innovation for the commercialization of a continuously tunable mode-hop-free laser based on his work in quantum cascade lasers.

Gerard Wysocki is an Assistant Professor of Electrical Engineering at Princeton University. He received his Ph.D. degree in physics in 2003 from Johannes Kepler University in Linz, Austria and his M.S. degree in electronics in 1999 from the Wroclaw University of Technology in Poland. Prior to joining Princeton University in 2008 he was a Faculty Fellow at Rice University in Houston, TX. He conducts research focused on the development of mid-infrared laser spectroscopic instrumentation for applications in trace gas detection and chemical sensing. His current research interests include development and applications of new tunable mid-infrared lasers, molecular dispersion sensing techniques for in-situ and remote chemical detection, and distributed wide area spectroscopic sensor networks. He published over thirty technical papers and co-authored over 70 presentations in the international conferences and meetings.

Frank K. Tittel is the Josephine S. Abercrombie Professor of Electrical Computer Engineering at Rice University, where he also holds a faculty appointment in the Department of Bioengineering. He obtained his bachelor, master, and doctorate degrees in physics from the University of Oxford in 1955 and 1959, respectively. From 1959 to 1967 he was a Research Physicist with General Electric Research and Development Center, Schenectady, New York. At G.E. he carried out early pioneering studies of dye lasers and high power solid state lasers. Since 1967 he has been on the faculty at Rice University in Houston, Texas. In 1973 and 1981 he was an Alexander von Humboldt Senior Fellow at the Max-Planck Institutes of Biophysical Chemistry, Göttingen, and Quantum Optics, Munich, respectively. He held visiting professor appointments at NASA Goddard Space Flight Center, University of Aix-Marseille, Keio University (Japan), and the Swiss Federal Institute of Technology (ETHZ). Current research interests include various aspects of quantum electronics, in particular laser spectroscopy, nonlinear optics, and laser applications in environmental monitoring, industrial process control, and medicine. He has published more than 350 technical papers and holds eight US patents in these areas. He is a Fellow of the IEEE, the Optical Society of America and the American Physical Society. He received a Doctor of Science (HC) degree from JATE University, Szeged, Hungary, in 1993, and he is an honorary Professor of the Harbin Institute of Technology, China since 1986. He is an Associate Editor of *Applied Physics B*, and a former Editor-in-Chief of *IEEE Journal of Selected Topics in Quantum Electronics* (1996–1998) and Associate Editor of the *IEEE Journal of Quantum Electronics*. He has served on numerous conference program committees such as CLEO, IQEC, and LACSEA.